VOLUME 23, 1961/62, No. 6 pp. 161-188 Published 13th March 1962

Philips Technical Review

DEALING WITH TECHNICAL PROBLEMS
RELATING TO THE PRODUCTS, PROCESSES AND INVESTIGATIONS OF
THE PHILIPS INDUSTRIES

ZONE MELTING OF OXIDES IN A CARBON-ARC IMAGE FURNACE

by C. KOOY *) and H. J. M. COUWENBERG *). 66.049.4:548-31:621.365.24

In solid-state research the method of heating in a radiation furnace, using a carbon arc as the primary source of heat, yields advantages similar to those of the conventional method of high-frequency heating. Unlike the latter, however, radiation heating can also be applied to materials of very high resistivity, which include many oxides. By means of special devices it is consequently possible to subject these materials to the process of zone melting, familiar from semiconductor technology (where it is applied in the special forms of zone refining and zone levelling). In this way large single crystals have been prepared from a series of oxides. The composition of the crystals proved to be reasonably close to the stoichiometric composition.

Technologists and experimenters early hit upon the idea of producing very high temperatures by means of a *solar furnace*, in which the sun's rays are focused into an intense image by a large parabolic mirror. An object placed in that image can be heated to extremely high temperatures, theoretically to the temperature of the sun itself. Towards the end of the 17th century Von Tschirnhaus in Dresden had several large lens systems built for this purpose [1]), with which he is believed to have achieved temperatures up to 3000 °C.

Solar furnaces are still used today [2]), partly because they are one of the means of making the sun's energy directly of service to man, partly because of the high temperatures which they bring within easy reach. Some of their additional advantages compared with conventional furnaces are: the atmosphere in which the charge is heated can be independent of the source of heat; the irradiation is confined to a very small area where melting can occur; as a consequence, the non-molten material can itself act as a "crucible" and there is no risk of the melt being contaminated by foreign matter from this source; finally, the temperature can be raised in an extremely short time and the charge kept under observation during the heating process.

Radiation heating shares these advantages with *RF induction heating*, which is therefore widely used in solid-state research, particularly for the zone melting of silicon and germanium [3]). RF heating falls down, however, where the material to be melted has been developed for the very object of causing minimum energy dissipation in high-frequency fields, as is the case with ferrites. More generally the same applies to materials that have a very high electrical resistivity, such as the oxides NiO, TiO_2 and others.

For the zone melting of such materials we have used the method of radiation heating with good results — although not with a solar furnace but with a *carbon-arc image furnace*. In our changeable climes the solar furnace scarcely commends itself for practical use, and the mechanism needed for the lens or mirror system to follow the course of the sun makes it relatively expensive as a laboratory instrument. The use of an intense terrestrial source

*) Research Laboratories, Eindhoven.

1) See page 182 of this number.

2) One of the world's largest installations, using a parabolic mirror of 90 m² surface area, has been erected in the Pyrenees. See: F. Trombe, Le laboratoire de l'énergie solaire de Mont-Louis, Bull. Soc. Chim. France 1953, pp. 353-368. See also: Applications thermiques de l'énergie solaire dans le domaine de la recherche et de l'industrie, Colloque international à Mont-Louis, June 1958, Centre National de la Recherche Scientifique, Paris (about 50 articles).

3) See J. Goorissen, Segregation and distribution of impurities in the preparation of germanium and silicon, Philips tech. Rev. **21**, 185-195, 1959/60.

of radiation, e.g. the carbon arc, instead of the sun's rays makes a much simpler construction possible, which still offers most of the advantages of the solar furnace. A description will be given here of an arc image furnace which has been in use for the zone melting of oxides in this laboratory for about two years. The working procedure will be discussed and some results mentioned [4]).

Description of the apparatus

The radiation from the carbon arc can be concentrated upon an object very effectively with an arrangement of two elliptical mirrors (see *fig. 1c*). This arrangement is better than one using a single elliptical mirror (fig. 1*a*), since the symmetrical path of the rays results in an image having less optical aberration and therefore a greater radiant flux in the focus used for heating. For practical purposes, two elliptical mirrors are preferable to two parabolic mirrors (fig. 1*b*) in view of the additional possibilities offered by the small cross-section

With an arrangement using two elliptical mirrors, Null and Lozier [6]) have shown that the radiant flux at the focus used for heating can reach 10 to 14 watt/mm^2 (depending on the type of carbons). This value is only slightly lower than the maximum value of about 15 W/mm^2 hitherto achieved in solar furnaces. With their apparatus Null and Lozier were able to melt small quantities of such materials as zirconium oxide (melting point 2970 °K), titanium carbide (3400 °K), tungsten (3680 °K) and even zirconium carbide (3800 °K).

The radiation source in our apparatus is a cinema-projection arc lamp (Philips type EL 4455). This lamp is already fitted with an elliptical mirror, which serves as one of the two mirrors for the arrangement shown in fig. 1*c*. The second mirror used is identical, see *fig. 2*. The diameter of the mirrors is about 36 cm, and the focal lengths are 14 and 68 cm. The carbons in the lamp are rated for an arc current of 80 A; the carbon feed is continuous and automatic.

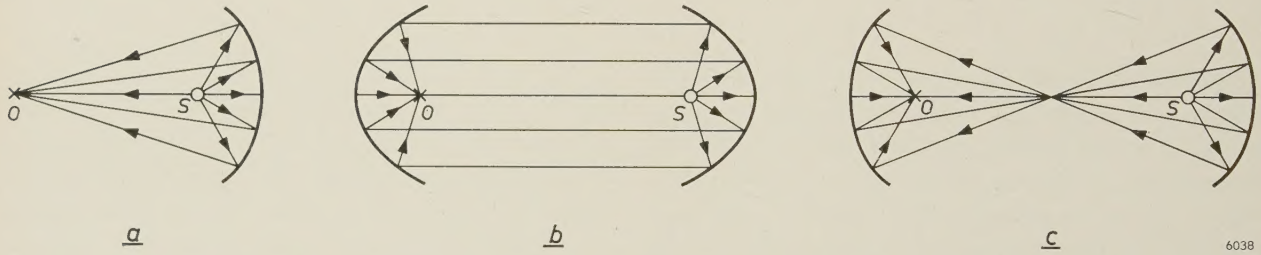

Fig. 1. Three possible mirror arrangements for heating an object *O* with the aid of a radiation source *S*.
a) Single elliptical mirror, with *S* and *O* in the two foci of the ellipse.
b) Two parabolic mirrors, with *S* and *O* each in the focus of one of the parabolas.
c) Two elliptical mirrors, so arranged that they have one focus in common and with *S* and *O* in the two other foci.

of the beam at the central "focus": diaphragms can easily be introduced near this point, or a plane mirror to alter the light path. The latter may be useful to avoid interrupting long heating periods when new carbons have to be fitted: in that case *two* carbon arcs are used and alternately ignited and focused on to the object by reversing the plane mirror [5]).

The radiant flux at the focus used for heating in this furnace has not been measured but is estimated to be roughly 5 W/mm^2. The temperatures obtainable depend to a marked extent, of course, on the absorption and reflection by the irradiated substance. If the material is transparent or highly reflecting, the actual increase in temperature will be slight. Glass, for example, hardly gets hot, and the fairly transparent Al_2O_3 (melting point 2320 °K) cannot be melted by the radiant flux mentioned — unless a little chromium is added to increase absorption. On the other hand NiO (melting point 2360 °K), which is a good absorber, is easily melted: a 5 mm thick sintered NiO rod melts within a few seconds of being placed in the focus. This incidentally is a

[4]) Similar equipment on the market (cf. [5])) has been used for a number of other applications. As far as we know, however, zone melting using an image furnace has hitherto only been applied to small quantities of organic compounds, i.e. with relatively low temperatures up to say 200 or 300 °C. The arrangement consisted of a single elliptical mirror; see E. F. G. Herington, Zone refining, Endeavour **19**, 191-196, 1960.

[5]) See R. E. De la Rue and F. A. Halden, Arc-image furnace for growth of single crystals, Rev. sci. Instr. **31**, 35-38, 1960. Technical particulars of the carbon-arc image furnace will be found in: P. E. Glaser, Imaging-furnace developments for high-temperature research, J. Electrochem. Soc. **107**, 226-231, 1960.

[6]) M. R. Null and W. W. Lozier, Carbon arc image furnaces, Rev. sci. Instr. **29**, 163-170, 1958.

good illustration of the speed at which the radiation furnace heats up its charge. Other oxidic materials, such as TiO_2 and $MnFe_2O_4$ (a spinel) are also readily melted.

The mechanism used for introducing the charge into the focus of our carbon-arc image furnace is specially designed for the purpose of zone melting and more specifically for zone melting by the *floating-zone technique*. Two rotatable holders, which grip two rods of the oxide to be melted, are mounted in a frame in such a way that the axes of the rods are vertically in line. The upper holder is capable of slight vertical displacement, and the whole frame can be shifted over a fair distance in the same direction. By moving the frame the tip of the lower oxide rod is introduced first into the focus and melted. Next, the upper rod is dipped into the molten tip, and the surface tension of the melt causes the formation of a molten zone between the two rods. The zone can now be made to move up and down the rods by lowering or raising the frame.

The material is heated only at the side of the nearer mirror. To prevent this unilateral heating from causing irregular solidification and melting of the moving zone, the holders of both rods are made to *rotate*. A rotational speed of 60 to 120 r.p.m. is found in general sufficient to produce a solid-liquid interface of good rotational symmetry. If moreover the two holders are rotated in opposite directions (as in the present case), the opposing motions of rotation at either side of the zone give rise in the melt to a stirring action, which promotes a uniform temperature distribution and a homogeneous composition. The surface tension of the melt is high enough in the case of the oxides mentioned to keep a zone between 5 and 10 mm long intact with rods about 5 mm thick. The zone length can be regulated by varying the arc current or by slightly defocusing the second elliptical mirror.

Since the oxidic materials in question are heated so quickly to their melting point, relatively high zone speeds are possible. For example, the molten zone in the rod of $MnFe_2O_4$ remained intact in our apparatus at a speed of 20 cm per hour. Normally we work at a zone speed of a few centimetres per hour.

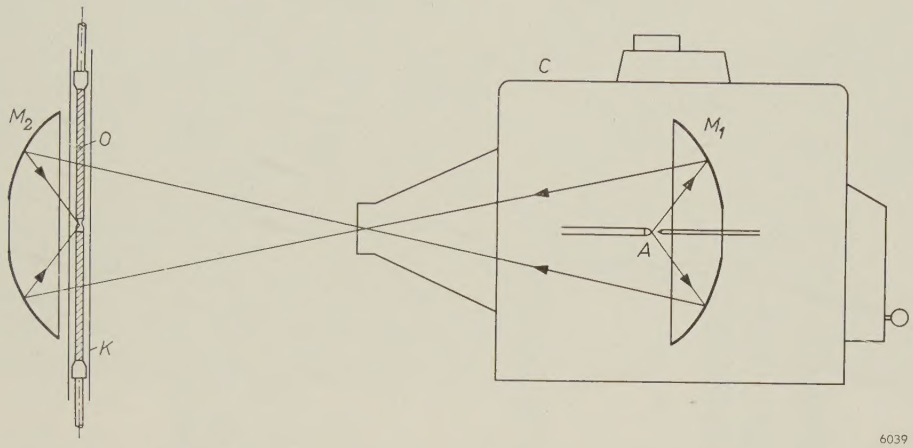

Fig. 2. Sketch of the carbon-arc image furnace. *C* cinema arc lamp, with carbon arc *A* and elliptical mirror M_1. The oxide rod *O* to be heated is situated in the proximate focal point of the second elliptical mirror M_2, and may be surrounded by a tube *K* of glass or quartz.

The rods can be surrounded by a tube of glass or quartz without interfering with the heating. In this way the entire process can be carried out in any desired gas atmosphere.

A photograph of the apparatus is shown in *fig. 3*, in which some of the details described can be seen.

Preparation of single crystals

The floating-zone technique offers an elegant possibility of producing single crystals. This method of producing crystals is widely used for metals, and has been developed into a highly refined technique for germanium and in particular for silicon, using RF heating. Hitherto, however, it has found scarcely any application for oxides of high melting point.

We have investigated the possibility of producing single crystals of oxides with a high melting point by zone melting in our carbon-arc image furnace. The results have proved to be very satisfactory. We have for example made single crystals of NiO

and TiO_2, and the following series of mixed crystals of $MnFe_2O_4$ with other compounds having the spinel structure:

$Mn_{1+x}Fe_{2-x}O_4$, with $x = -0.1$ or 0 or 0.1 or 0.2;

$MnTi_xFe^{II}_xFe^{III}_{2-2x}O_4$, with $x = 0.15$ or 0.30 or 0.45;

$MnTi_{0.15}Co_{0.15}Fe_{2.7}O_4$;

$Mg_{0.45}Mn^{II}_{0.55}Mn^{III}_{0.23}Fe_{1.77}O_4$.

The starting material used was obtained by prefiring powdered metal oxides, mixed in the right proportions, and by pressing these prefired powders into the shape of rods and sintering them. The sintered rods are still porous but sufficiently easy to handle, and have enough resistance to thermal shock to withstand zone melting without disintegrating.

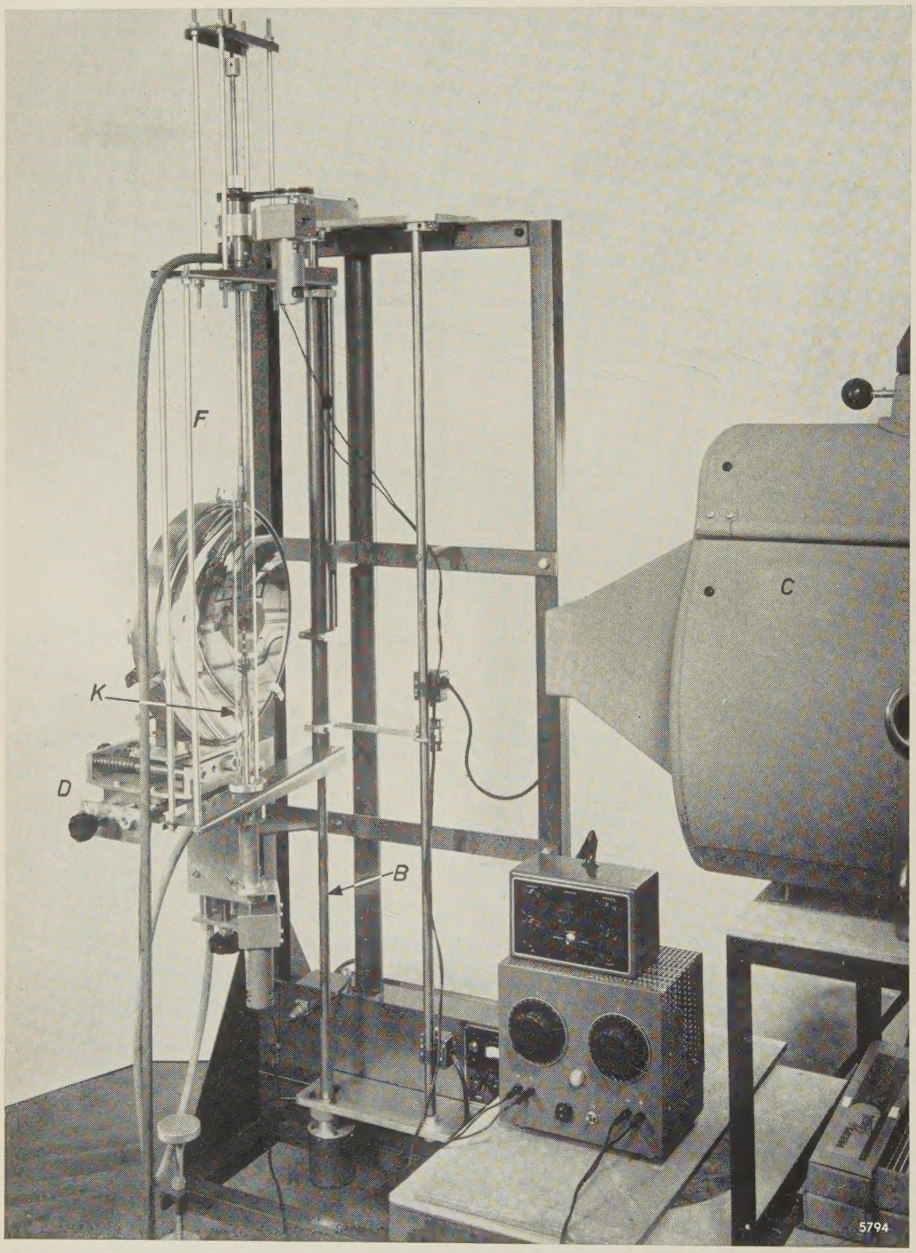

Fig. 3. Carbon-arc image furnace used in Philips laboratories at Eindhoven for the zone melting of oxides. Partly visible on the right is the cinema arc lamp *C* (type EL 4455), which has a built-in elliptical mirror as condenser. On the left can be seen the second elliptical mirror, mounted on a carriage *D*, adjustable in three directions. In the upper and lower parts of the frame *F*, which can be shifted vertically at variable speed along the guide rod *B*, are mounted on their bearings the rotary holders in which the oxide rods are clamped. The rotational speed of each holder is independently regulated by the lower control box, the movement of the frame by the upper one. Surrounding the oxide rods is a quartz tube *K*, to both ends of which rubber tubing is connected through which the gas in which the zone melting process is carried out is admitted to the tube.

Our crystal-growing techniques are similar to the standard ones as applied, for instance, to silicon. The growing crystal is initially narrowed to a very small diameter by increasing the distance between the two rods. Pieces of the single crystal thus produced may later be used as seeds for growing further single crystals. The total length of the single crystals obtained is limited by the burning life of the carbons (we have not yet used interchangeable carbon arcs, see above). At currents from 50 to 70 A this is between two hours and half an hour which, at a zone speed of a few centimetres per hour, yields crystals several centimetres long — sufficient for most purposes in solid-state research. Some of these single crystals can be seen in *fig. 4*. *Fig. 5* shows the molten zone during the growth of a single crystal of $MnFe_2O_4$.

The processes of zone melting and crystal-growing are much more complex for oxidic compounds than for elements such as Ge and Si, owing to the fact that the oxides may decompose and the equilibrium pressure of the oxygen in an oxide is critically dependent on temperature. The partial pressure

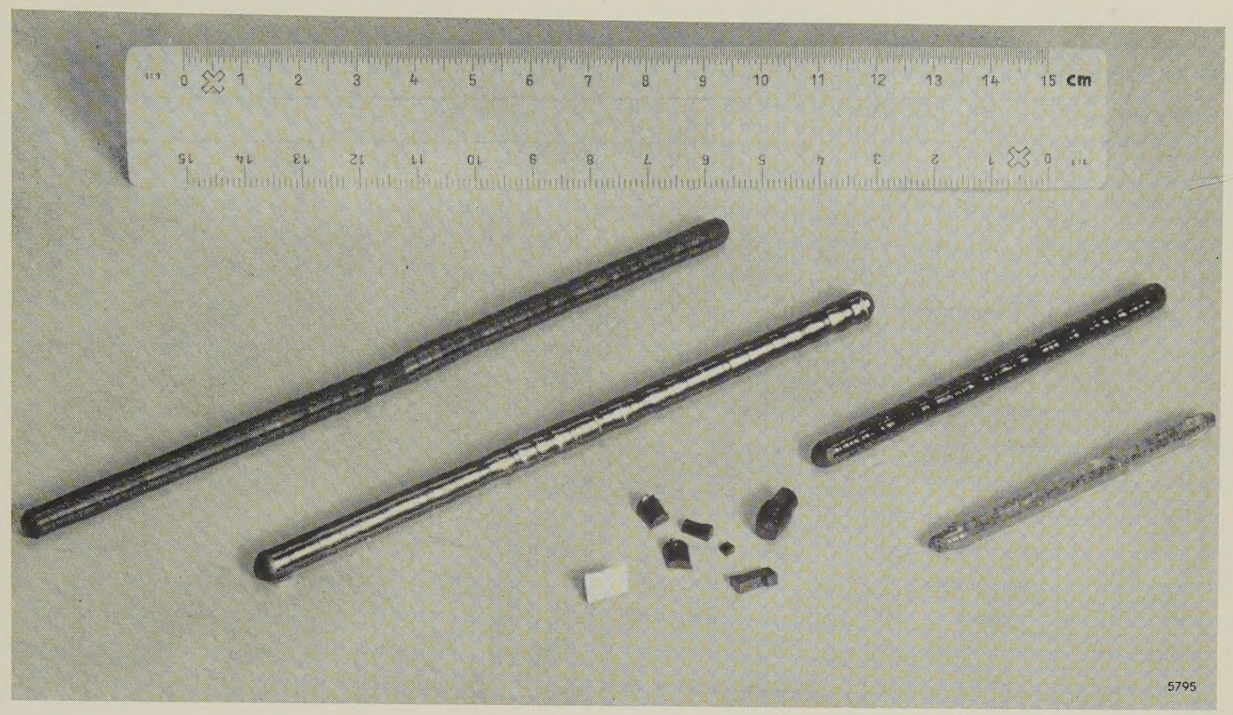

Fig. 4. Some monocrystalline rods of oxides produced in different atmospheres with the apparatus described. The zone speed in all cases was 6 cm per hour. From left to right: $MnFe_2O_4$ in air; $Mn_{1.1}Fe_{1.9}O_4$ in nitrogen with 0.2% oxygen; $Mn_{1.2}Fe_{1.8}O_4$ in nitrogen with 0.2% oxygen; TiO_2 in air. In the foreground are some fragments of an NiO rod, showing good cleavage planes; this rod was grown in pure oxygen.

chosen for the oxygen in the gas atmosphere will prevent both oxidation and decomposition at one temperature only. Within the molten zone the temperature is fairly constant because of the stirring effect caused by the rotation, but in the solidified part the temperature decreases very steeply in the axial direction. In traversing the zone, therefore, the material is bound to be successively reduced and oxidized.

When zone-melting NiO in air, for example, a considerable reduction occurs in the melt: upon abrupt cooling the melt can be shown to contain metallic nickel. Nevertheless, the material that crystallizes from the melt is almost exactly stoichiometric NiO, and the cooled rods are even slightly oxidized. When TiO_2 is zone-melted in air, the material solidifying from the melt is the reduced black modification which, during cooling, is completely re-oxidized into the light-yellow form of virtually stoichiometric TiO_2. As our last example we mention $MnFe_2O_4$ and the substituted manganese ferrites referred to above: when these are zone-melted in air the outer layer oxidizes during cooling. After removal of this skin, however, the core is again found to have a composition which is in fairly good agreement with the proportions by weight of the

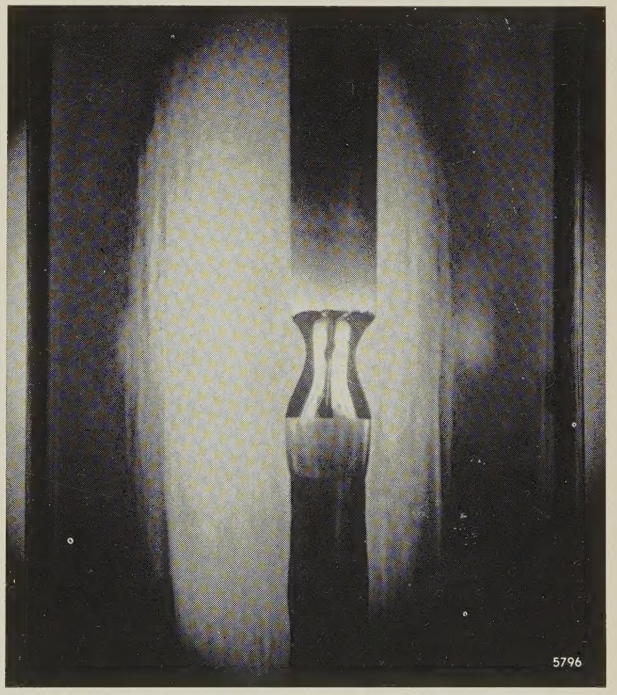

Fig. 5. Molten zone, photographed through the 3.5 cm wide quartz tube, during the growth of a single crystal of $MnFe_2O_4$. The frame with both rods is moving slowly downwards, which in effect means that the zone in the material moves upwards. The part above the zone is the sintered polycrystalline rod, 5 mm thick, and the part below is the solidified single crystal.

oxides in the sintered rods. When these manganese ferrites are zone-melted in nitrogen plus 0.2% oxygen, there is scarcely any oxidation of the outer layer (cf. fig. 4).

Thus, in spite of the complicating factor of decomposition, it is possible by zone-melting these oxides to produce single crystals that show no marked deviation from the stoichiometric composition. This applies to the crystal rod as a whole, since the constant supply of fresh material to the melt soon gives rise to a stationary state during the actual process of zone melting. This contrasts with two other methods of producing oxide crystals, namely the Bridgeman-Stockbarger method and the flux method [7]), where a gradual change in the chemical composition is unavoidable during crystal growth. Yet another method, based on the old Verneuil process [7]), has in common with zone melting the advantage of reaching a steady state, after which the composition of the solidifying material remains in principle constant. This process can also be carried out with radiation heating [5]), making a free choice of atmosphere possible. In the Verneuil process, however, the preparation of the starting material involves many more difficulties than in the method of zone melting described here.

In conclusion, mention may be made of a problem that arises in our process, and which is connected with the above-mentioned high temperature gradient in the material immediately after solidification. This is an inherent feature of the highly localized heating in the radiation furnace, the gradient being increased by the low thermal conductivity of many oxides. True, the local temperatures in the material cannot be accurately measured: the results found with the optical pyrometer (the only feasible method of measurement in this case) are difficult to interpret owing to the reflection of the intense light from the carbon arc. It may be assumed, however, that axial temperature gradients occur of the order of 1000 °C per cm. At a zone speed of 5 cm per hour this means that the single crystal actually cools down at a rate of roughly 100 °C per minute. Owing to the relatively low plastic deformability of the oxides, this rapid cooling often gives rise to *cracks* in the single crystals. If one wishes to avoid this, without unduly sacrificing the rate of growth, one must e.g. use additional heat sources to keep the solidified material longer up to temperature.

[7]) See e.g. F. W. Harrison, The growth of oxide single crystals containing transition metal ions, Research **12**, 395-403, 1959.

Summary. For the purpose of zone-melting oxides possessing a high electrical resistivity the use of RF induction heating — as applied to silicon and germanium — is not suitable. Such oxides can be effectively zone-melted, however, with the aid of radiation heating. An apparatus employed for this purpose is described, in which two elliptical mirrors produce an image of an intense carbon arc, and an oxide rod to be melted is placed in this image. The floating-zone technique is applied, so that the equipment is eminently suited for producing single crystals of oxides having a high melting point. The authors describe the preparation of rod-shaped single crystals of NiO, TiO_2, $MnFe_2O_4$ and of various substituted manganese ferrites. The composition is constant throughout the single-crystal rod and is in good agreement with the stoichiometric composition.

INFLUENCE OF THE NON-LINEAR BEHAVIOUR OF A RECORDING INSTRUMENT ON THE PROPERTIES OF A CONTROL SYSTEM

by C. H. LOOS *).

621-53.001:621.317.7.087.6

Pursuant to the articles on the application of control theory to linear systems published in the two preceding numbers of this journal, the article below deals with an element which behaves non-linearly when the input signal undergoes very rapid variations. In qualitatively analysing the stability characteristics of a control loop containing this element, use is made of a rule of thumb formulated in the second of the articles mentioned. The surprising conclusion is that the stability of the control loop in question is not a monotonic function of the speed of variation, but shows a minimum.

Introduction

For measuring and recording important variables in industrial plants, increasing use is being made of recording instruments (recording millivoltmeters) whose operation is based on automatic compensation of the measured quantity (voltage) by means of a servomechanism. Fundamentally, the circuit of these instruments stems from Poggendorf's well-known compensation method (*fig. 1a*), except that the null instrument here is replaced by an amplifier which drives the motor that moves the sliding contact of the potentiometer (see fig. 1*b*). Attached to the sliding contact is a stylus or pen. Non-electric quantities to be measured are first converted into an electrical signal.

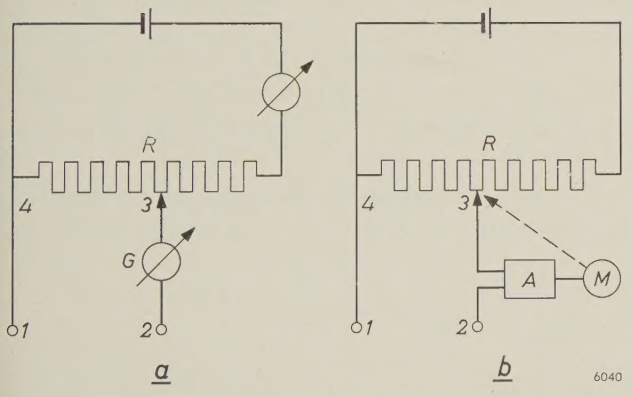

Fig. 1. *a*) Poggendorf compensation method of measuring an e.m.f. The voltage is applied to the terminals *1* and *2*. The contact *3* is then shifted until the highly sensitive meter *G* no longer shows a deflection. The potential difference between points *3* and *4* is then equal to the e.m.f. to be measured and can be calculated from the current flowing through *R* and the resistance between *3* and *4*.
b) In a recording instrument, *R* is a potentiometer whose sliding contact is moved by a motor *M*. The latter is fed by the potential difference between *2* and *3*, highly amplified by *A*. As soon as the potential difference is zero, the sliding contact remains stationary.

Frequently the recorded quantities also have to be automatically controlled, in which case the recording instrument itself can sometimes be used as part of the controller, i.e. as an amplifier. For this purpose a second potentiometer is employed, which is fed with a constant voltage much higher than the voltage across the measuring potentiometer, and whose sliding contact moves synchronously with that of the other. In this way a gain of e.g. 5000× can readily be achieved, offering a particularly simple method of effecting the control action.

A recording instrument thus modified behaves as a linear element only when the changes in the input signal are slow enough for the sliding contact (the pen) to follow. In this article we shall examine what happens when this condition is not fulfilled. It will be shown that instability effects may arise in a control loop which contains, in addition to the recording instrument, two elements having the transfer function $(1 + j\omega\tau)^{-1}$. If the recorder were an ideal amplifier, a control system of this kind ought to be stable for every value of the loop gain [1]). Remarkably enough, the extent to which the stability is endangered — we shall express this presently in a more rigorous form — does not increase monotonically with the discrepancy between the desired speed of the pen and the maximum possible speed. In fact, where this discrepancy is very large, the danger of instability decreases!

The sliding contact will no longer follow a varying signal when the amplifier *A* (fig. 1*b*) is overdriven. Irrespective of the magnitude of the potential between *2* and *3*, the amplifier

*) Research Laboratories, Eindhoven.

[1]) Examples of control loops with linear elements will be found in the article by M. van Tol, Philips tech. Rev. **23**, 109, 1961/62 (No. 4), where the transfer function is also discussed. The relation between loop gain and stability is dealt with by M. van Tol in Philips tech. Rev. **23**, 151, 1961/62 (No. 5).

then delivers its maximum output signal and the pen consequently moves at a constant speed. Even when the amplifier is not overdriven, the pen does not of course follow a varying signal exactly: the motor can only turn when the potential between *2* and *3* differs from zero. The deviation is smaller the higher the gain factor of A; theoretically it approaches zero for an infinitely high gain factor. If a *constant* signal is applied between *1* and *2*, and the motor behaves like an ideal integrator, the deviation will of course be zero in the long run.

With the aid of two figures we shall now try to show qualitatively the way in which the output voltage of the instrument varies when the variations in the input voltage are too fast. We at once introduce the approximations necessary to simplify the theoretical treatment of the instrument's behaviour. The most general case is represented in *fig. 2*. The

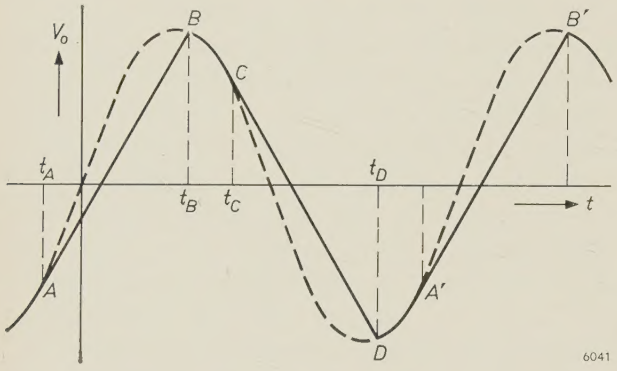

Fig. 2. Output voltage of a recording instrument adapted as a controller, when the maximum speed at which the input signal varies is too fast for the pen to follow. The pen follows the input signal only between B and C (and D and A', etc.). Outside these regions the pen moves uniformly at its maximum speed.

broken curve represents the input signal and the solid line the output signal. For convenience the gain is assumed to be unity. When the input-signal variations are too fast for the pen to follow, the pen moves at a constant speed (portion AB). This continues until the speed of variation has dropped sufficiently to allow the pen to catch up again (point B). The pen now follows the variation of the input voltage until (at point C) the signal again changes too rapidly. Thereupon the output signal again varies linearly with time (portion CD) and so on.

If we now increase the frequency or the amplitude of the output signal, points B and C etc. come closer together, until finally the signal acquires a triangular waveform (*fig. 3*).

Summarizing, then, we note that with rising frequency and/or amplitude the gain is initially linear. When a certain limit is exceeded, we obtain the case represented in fig. 2, and finally, after passing a second limit, the case in fig. 3. We shall now put this into mathematical form, after which we shall examine the behaviour of the instrument as an element in a control loop, with the aid of *describing functions*. In this method the problem is treated as if the element were a linear one, the output signal following from a sinusoidal input signal being approximated by its fundamental Fourier component. For these sinusoidal signals we can then establish a transfer function — the describing function — in the same way as for linear elements. Unlike the transfer function of a loop consisting solely of linear elements, however, this describing function may contain the amplitude as well as the frequency of the input signal.

The describing function is especially useful for analysing the stability of a control loop containing a non-linear element. Since the higher Fourier components of an output signal whose frequency is near the cut-off frequency are usually strongly attenuated in the other elements of the loop, the signal when it appears again at the input of the non-linear element, having passed once around the loop, has in fact become virtually sinusoidal, and may to a very good approximation be regarded as solely due to the fundamental Fourier component.

Calculation of the transfer function

To calculate the transfer function of the recorder we start from a sinusoidal input signal of amplitude U. Disregarding the limited speed of the recorder, we consider the instrument to be an ideal amplifier having a gain factor A. Since the magnitude of A has no effect on the behaviour of the instrument — although of course it does affect the control loop to which it belongs — we shall henceforth assume A to be equal to unity.

The rate of change of the input signal $U \sin \omega t$ is $\omega U \cos \omega t$. As long as ωU is smaller than the

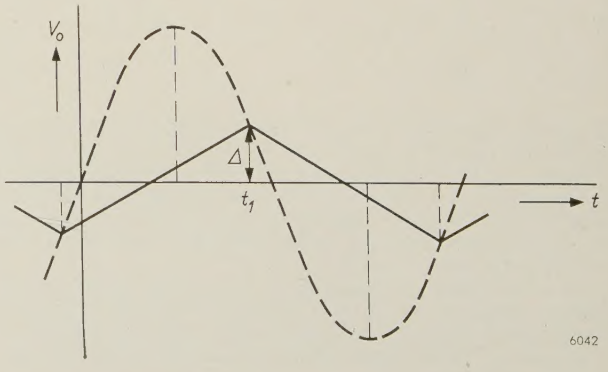

Fig. 3. When the maximum speed at which the input signal changes substantially exceeds the maximum writing speed, the output signal has a triangular waveform.

value corresponding to the maximum speed B of the pen, the behaviour of the instrument is linear.

We shall first consider the case represented in fig. 3, where the pen is no longer able to follow the input signal at all, and the output signal has a triangular waveform. The slope of the straight lines is $+B$ and $-B$ respectively, and the amplitude Δ of the signal (half the peak-to-peak value) is $\pi B/2\omega$. The first Fourier component (first harmonic) of a triangular signal of amplitude Δ (see appendix) is:

$$\frac{8\Delta}{\pi^2} \sin(\omega t + \varphi). \quad \ldots\ldots \quad (1)$$

The amplitude ratio of the first harmonics of output and input signals is thus:

$$\frac{4}{\pi} \times \frac{B}{\omega U}. \quad \ldots\ldots\ldots \quad (2)$$

The phase angle φ is quickly found when it is remembered that the peak value of the output signal, and hence of its first harmonic, occurs at the moment at which the input signal (in the second quadrant) also has the value $\pi B/2\omega$, and that the peak value of the input signal occurs when $\omega t = \pi/2$. It follows from this that:

$$\varphi = \frac{\pi}{2} - \left(\pi - \text{arc sin}\frac{\pi B}{2\omega U}\right) = -\frac{\pi}{2} + \text{arc sin}\frac{\pi B}{2\omega U}. \quad \ldots\ldots \quad (3)$$

Before considering the case of fig. 2, we shall consider what are the "limits" mentioned above. We have seen that the behaviour of the instrument is linear if $\omega U < B$, i.e. if $B/\omega U > 1$.

The case of fig. 3 — triangular output voltage — occurs where $-\omega U \cos \omega t_1 > B$, that is where $\omega U \cos \text{arc sin} \dfrac{\pi B}{2\omega U} > B$, i.e. where

$$\sqrt{1 - \left(\frac{\pi B}{2\omega U}\right)^2} > \frac{B}{\omega U}.$$

This is the case when

$$\frac{B}{\omega U} < \frac{1}{\sqrt{1 + \pi^2/4}},$$

i.e. when

$$\frac{B}{\omega U} < 0.538.$$

The case of fig. 2 thus occurs in the region

$$0.538 < \frac{B}{\omega U} < 1. \quad \ldots\ldots \quad (4)$$

If we now calculate the first Fourier component of the output signal when the latter is partly sinusoidal and partly linear with respect to time (see appendix), we find for the amplitude of the first sine term:

$$b_1 = \frac{U}{\pi}\{\pi - \text{arc cos}\, p - k(p) - \sin k(p) \cos k(p) + p\sqrt{1 - p^2} + 2p \sin k(p)\}, \quad \ldots \quad (5)$$

and for that of the first cosine term:

$$a_1 = \frac{U}{\pi}\{\cos k(p) - p\}^2, \quad \ldots \quad (6)$$

where $p = B/\omega U$ and $k = \omega t_B$ (cf. fig. 2). From this we can directly derive the amplitude ratio $(\sqrt{a_1^2 + b_1^2}/U)$ and the phase shift $(\text{arc tan}\, a_1/b_1)$ for the relevant range of p values. Combining the result with those for the regions $p > 1$ and $p < 0.538$, and plotting a Bode diagram — with the quantity $\omega U/B$ or $1/p$ as the abscissa — we arrive at *fig. 4*. As can be seen, the characteristics closely resemble those of a linear element having one time constant τ_R of magnitude $\pi U/4B$. This time constant is thus proportional to the amplitude of the input signal and inversely proportional to the maximum writing speed.

A characteristic difference is that for p values greater than unity the gain is exactly constant and the phase shift exactly zero. In this region the

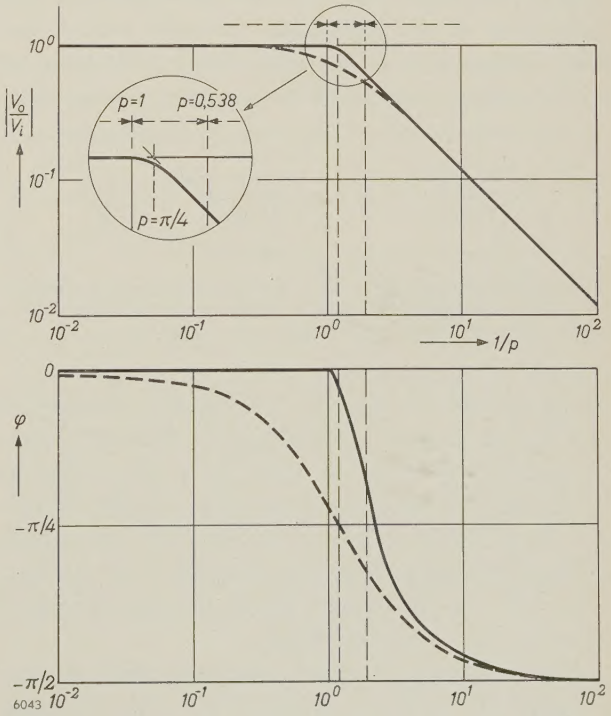

Fig. 4. Bode diagram representing the frequency-response characteristics of a recording instrument. The quantity $1/p$ $(= \omega U/B)$ is plotted as the abscissa. The curves may be approximated by those of an element having a single time constant τ_R of the value $\pi U/4B$ (broken lines).

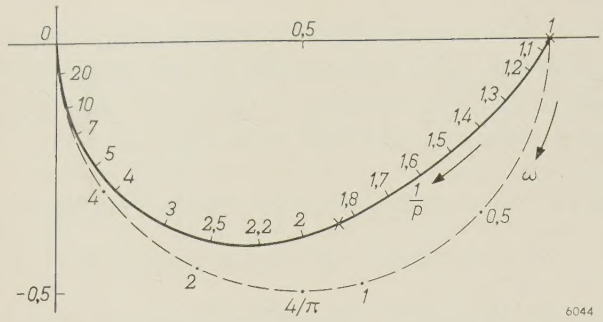

Fig. 5. Nyquist diagram appertaining to fig. 4. The quantity $1/p$ is again chosen as the variable in order to draw one curve instead of a set of curves. The crosses mark the points $p = 1$ and $p = 0.538$. As in fig. 4, the broken curve relates to an element having the transfer function $(1 + j\omega\pi U/4B)^{-1}$. The figures given beside this curve relate, of course, to ω.

instrument does not behave like an element with a single time constant but in fact like an ideal amplifier. The relevant Nyquist diagram is shown in *fig. 5*. This too is represented in such a way that a point on the curve is not applicable to a certain value of ω but to $1/p$. It should be noted that all points for which $0 < 1/p < 1$ coincide on the real axis.

A recording instrument in a control loop with two time constants

We shall now examine the characteristics of a control loop as shown in *fig. 6*. Here R and A together constitute the recorder; R represents the behaviour of the instrument as such and A the gain independent of R, which is solely determined by the voltage applied to the second potentiometer.

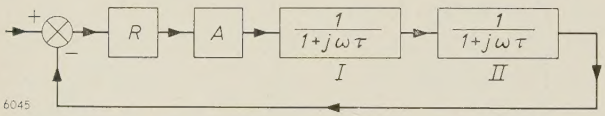

Fig. 6. Block diagram of a control loop consisting of a recorder R, an ideal amplifier with gain factor A, and two elements whose transfer function is $G(j\omega) = (1 + j\omega\tau)^{-1}$.

Blocks I and II both have a transfer function of the form $(1 + j\omega\tau)^{-1}$, but markedly different values of τ. Where $p > 1$, the recorder behaves like an ideal amplifier and the control loop is stable. Where $p < 1$, however, R also contributes to the phase shift, which may therefore in principle be greater than 180°, so that instability may occur. We shall examine this point presently.

First, however, we shall emphasize that, for the purposes of stability considerations, the situation in a loop containing a nonlinear element differs somewhat from that of a loop containing nothing but linear elements. For in this case the Nyquist diagram does not contain simply one curve, which may or may not enclose the point (—1,0), but a set of curves whose parameter is an amplitude — in our case the amplitude of the signal (which may consist only of noise) appearing at the input of the recorder. To be sure of stability, the loop gain should be chosen such that that curve in the complete set of curves which cuts off the largest section of the negative real axis does not enclose the point (—1,0). If that section has no finite value, then stability is out of the question.

A good qualitative insight into the behaviour of the control loop in fig. 6 can be obtained by using the rule of thumb arrived at in the above-mentioned article [2]). This stated that in a control loop which, besides an ideal amplifier, contained solely elements having the transfer function $G(j\omega) = (1 + j\omega\tau)^{-1}$, the maximum permissible loop gain A_{max} is equal to τ_1/τ_2. Here τ_1 is the longest and τ_2 the next longest time constant. If $A = \tau_1/\tau_2$, then the gain drops to unity at the second break in the double-logarithmic amplitude characteristic, i.e. at a phase shift of 135° (90° due to the block with τ_1 and 45° due to that with τ_2). Although the break in the case of the recorder corresponds to a phase shift somewhat smaller than 45°, that does not affect the validity of the argument.

If τ_R is initially the longest of the time constants ($\tau_1 = \tau_R$), then τ_R determines the position of the *first* break (*fig. 7a*) and an increase in U — we call the initial value U_1 — leads to greater stability, and a decrease to reduced stability. If τ_R is the next largest time constant (fig. 7*b*), then τ_R determines the position of the *second* break in the curve, and the stability reacts in precisely the opposite way to variations in U.

If we now let the amplitude U pass through a range of values such that τ_R begins with the next largest time constant and ends with the largest, and if we start from a stable state ($A = \tau_1/\tau_R$), we then see that as U increases the stability decreases — and may finally result in instability — but that the stability of the system increases again as soon as τ_R has become the largest time constant. The stability is therefore not a monotonic function of U, but shows a minimum when τ_R is roughly equal to the longer of the two fixed time constants.

An important consequence of this effect is that when a control loop of the type in fig. 6 becomes unstable it does not start to oscillate with ever-increasing amplitude, but enters into a *stationary* state (see below). By measuring the amplitude and frequency occurring in this state for various values of the two fixed time constants we have been able to verify experimentally the theory described above.

We shall work this out quantitatively for the case where the two fixed time constants are identical. Let the transfer function of the recording instrument be approximately $(1 + j\omega\tau_R)^{-1}$ where $\tau_R = \pi U/4B$ (see above), then the transfer function KG of the entire (open) control loop is given by:

$$KG = \frac{A}{(1 + j\omega\tau)^2 (1 + j\omega\tau_R)} = \frac{A}{(1-\omega^2\tau^2-2\omega^2\tau\tau_R) + j(2\omega\tau + \omega\tau_R-\omega^3\tau^2\tau_R)} .$$

The Nyquist diagram for this function, for the case where $A = 10$ and both fixed time constants are equal to one second, is shown in *fig. 8*. Here again, there is not just one curve but a set of curves with τ_R as parameter. The three curves shown relate to cases where τ_R is equal to 0.1, 1.0 and 10 seconds,

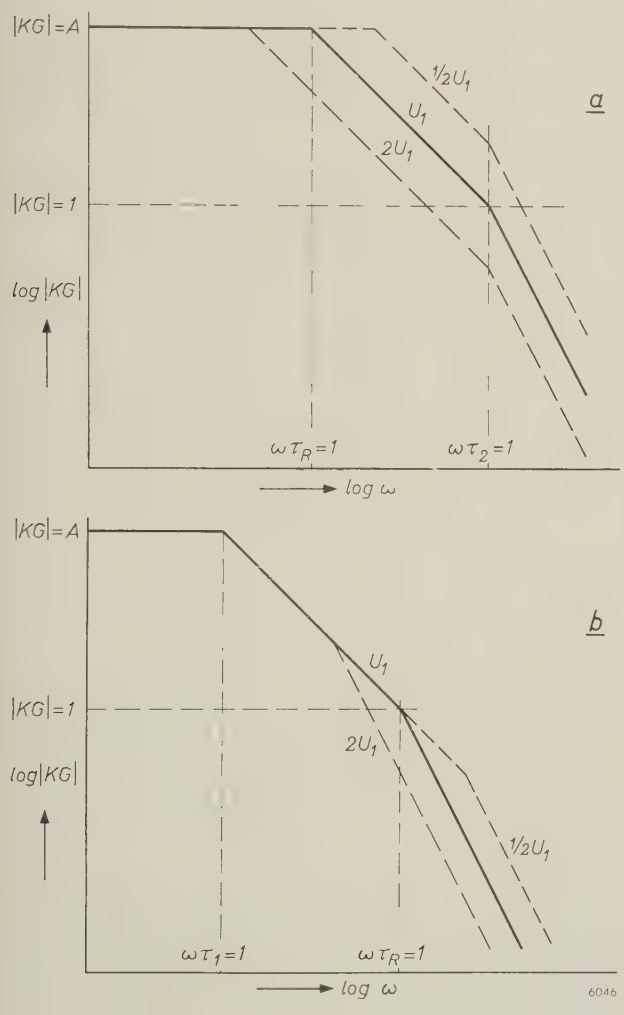

Fig. 7. Bode diagram of the control loop in fig. 6, approximated by straight lines. *a*) The time constant τ_R of R is the longest of the three time constants. When the amplitude U increases (the other parameters remaining constant) the first break shifts to the left and the gain at $\omega = 1/\tau_2$ decreases, as a result of which the stability increases. *b*) τ_R is the next largest time constant and determines the position of the second break in the curve. With increasing amplitude the stability decreases.

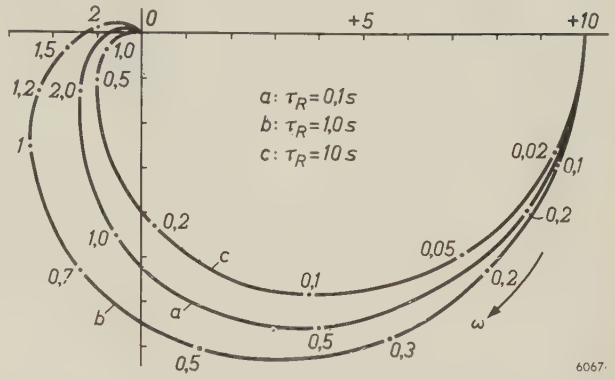

Fig. 8. Nyquist diagram of the control loop in fig. 6, for the case where the two fixed time constants are both 1 second and A is 10. A set of curves is found whose parameter is the time constant τ_R of the recorder. For $\tau_R = 0.1$ sec and 10 sec the closed loop is stable; for $\tau_R = 1.0$ sec it is unstable. The figures beside the curves again give the relevant values of ω.

respectively. As can be seen, the closed loop *is* stable in the two extreme cases, but not when τ_R is 1 second.

The behaviour of the stability as a function of τ_R — i.e. as a function of U/B — can be derived from the displacement of the point where the KG curve intersects the negative real axis. For this purpose we equate the imaginary part with zero:

$$\omega(2\tau + \tau_R - \omega^2\tau^2\tau_R) = 0 . \quad . . \quad (7)$$

The curve therefore intersects the negative real axis ($\omega \neq 0$) when:

$$\omega^2 = \frac{2\tau + \tau_R}{\tau^2\tau_R} . \quad . . . . . \quad (8)$$

The coordinate of the point of intersection is:

$$\frac{A}{1 - \{\tau^2 + 2\tau\tau_R\}\left\{\frac{2\tau + \tau_R}{\tau^2\tau_R}\right\}} = \frac{A\tau\tau_R}{-2(\tau+\tau_R)^2} . \quad (9)$$

It follows directly from eq. (9) that the point of intersection tends to the origin when τ_R is very small or very large. The absolute value of the real coordinate is maximum when $\tau_R = \tau$. Substituting this in eq. (9) we find that this maximum value is equal to $A/8$. Where $A > 8$, as in the example of fig. 8, there is therefore a region of τ_R values at which the system is unstable. The limits τ_R' and τ_R'' of that region can be calculated with the aid of eq. (9). We find

$$\tau_R' = \tfrac{1}{4}\tau\{(A-4) - \sqrt{A(A-8)}\}, \quad (10a)$$

and

$$\tau_R'' = \tfrac{1}{4}\tau\{(A-4) + \sqrt{A(A-8)}\}. \quad (10b)$$

If we let τ_R — or the amplitude U, where B is fixed — increase from a low value, the system begins

to oscillate as soon as τ_R exceeds the value τ_R'. As a result, the amplitude goes on increasing of its own accord to a value corresponding to τ_R''. The system then remains oscillating at this amplitude with a frequency given by:

$$\omega^2 = \frac{2\tau + \tau_R''}{\tau^2\,\tau_R''}. \quad . \quad . \quad . \quad . \quad (11)$$

Experiments have shown the measured oscillation frequencies and amplitudes to be in good agreement with the relations derived theoretically.

Appendix: Calculation of the first Fourier components of the output signal

The amplitudes b_n and a_n of the nth sine and cosine terms in the Fourier expansion of the periodic function $f(x)$ are given by the equations:

$$b_n = \frac{1}{\pi}\int_{-\pi}^{+\pi} f(\xi)\sin n\xi\,d\xi, \quad . \quad . \quad . \quad . \quad . \quad (12a)$$

and

$$a_n = \frac{1}{\pi}\int_{\pi}^{+\pi} f(\xi)\cos n\xi\,d\xi. \quad . \quad . \quad . \quad . \quad . \quad (12b)$$

Writing the nth harmonic in the form

$$\sqrt{a_n^2 + b_n^2}\,\sin(\omega t + \varphi_n),$$

we find that the phase angle φ_n is equal to arc tan a_n/b_n. If $f(x)$ cannot be described by one analytical function in the whole region from $-\pi$ to $+\pi$, the integrals in (12) must be split into separate integrals whose limits are those within which the relevant expression for $f(x)$ is applicable. In calculating the first Fourier component of the triangular output voltage (fig. 3) we shall disregard the phase — which has already been found by other means — and choose the zero point of the time axis so as to enable us to use a sine series. We then find

$$b_1 = \frac{2}{\pi}\int_0^{\pi/2}\frac{2\Delta}{\pi}x\sin x\,dx + \frac{2}{\pi}\int_{\pi/2}^{\pi}\frac{2\Delta}{\pi}(\pi - x)\sin x\,dx = 8\Delta/\pi^2. \quad (13)$$

In order to calculate the first Fourier component of the partly sinusoidal and partly linear output signal (the case of fig. 2) we have to ascertain the moments at which a particular part changes to the next. We shall first consider the transition from a sinusoidal to a linear part (fig. 2, point A). For the relevant moment of time t_A we can write:

$$\omega U\cos\omega t_A = B,$$

or

$$\omega t_A = -\arccos B/\omega U. \quad . \quad . \quad . \quad . \quad . \quad . \quad (14)$$

Putting $B/\omega U = p$, the value V_A of the output voltage V_0 that occurs at $t = t_A$, and which is equal to $U\sin\omega t_A$, can be reduced using eq. (14) to:

$$V_A = -U\sqrt{1-p^2}. \quad . \quad . \quad . \quad . \quad . \quad . \quad (15)$$

The equation of the line section AB is then:

$$V_0 = -U\sqrt{1-p^2} + B(t + \frac{1}{\omega}\arccos p). \quad . \quad . \quad . \quad (16)$$

The point B where the output voltage again becomes sinusoidal is found by ascertaining the value of t at which the line defined by (16) intersects the sinusoidal line:

$$U\sin\omega t_B = -U\sqrt{1-p^2} + B(t_B + \frac{1}{\omega}\arccos p). \quad (17)$$

Putting $\omega t_B = k$, equation (17) transposes to:

$$\sin k + \sqrt{1-p^2} = +kp + p\ \arccos p. \quad . \quad . \quad (18)$$

This equation cannot be solved analytically, and therefore no formula can be derived from it for t_B. We have therefore adopted a graphic solution. In *fig. 9* can be seen how k $(=\omega t_B)$ varies with p $(=B/\omega U)$ in the region $0.538 < p < 1$. The four expressions for $f(\xi)$ to be used here, and the limits between which these expressions are valid, are given in the following table.

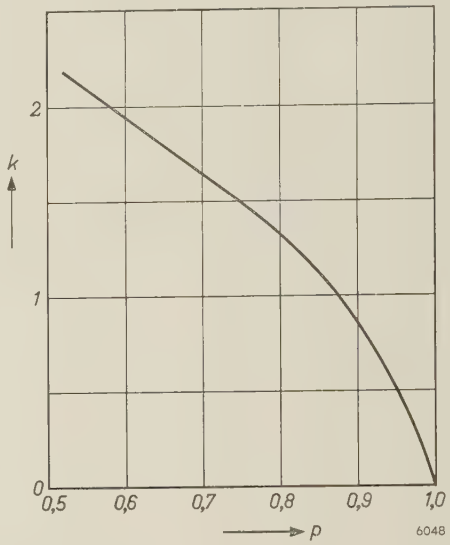

Fig. 9. Variation of the quantity k $(=\omega t_B)$ as a function of p $(=B/\omega U)$.

function	lower limit $\omega t =$	upper limit $\omega t =$
$Bt + Up\arccos p - U\sqrt{1-p^2}$	$-\arccos p$	k
$U\sin\omega t$	k	$\pi - \arccos p$
$-Bt + Up\pi - Up\arccos p + U\sqrt{1-p^2}$	$\pi - \arccos p$	$\pi + k$
$U\sin\omega t$	$\pi + k$	$2\pi - \arccos p$

The fact that k can only be calculated numerically does not make it impossible to carry out the integrations analytically (see (5) and (6)). Numerical calculation is required only when it is necessary to determine the variation of the coefficients a_1 and b_1 with p.

Summary. When the speed at which the input signal varies exceeds a certain value, the pen of a recorder is no longer able to follow the signal, but moves uniformly at its maximum speed B. In such a case the recording instrument may no longer be regarded as a linear and lag-free element. The frequency-response characteristics found when the output signal is approximated by its first Fourier component are found to resemble closely those of an element having a single time constant. The value of this time constant, however, is here proportional to the amplitude U of the input signal and inversely proportional to B. When this element is included in a control loop having a further two time constants, the stability of the loop is a function of U. The maximum stability is found at very small *and* at very large values of U.

CIRCUITS FOR DIFFERENCE AMPLIFIERS, II

by G. KLEIN*) and J. J. ZAALBERG van ZELST*). 621.375:621.317.725.083.6

*Part II of this article deals with some of the problems that arise in the application of the circuits discussed in part I**). Some other uses for difference amplifiers are described, in particular as an "electronic voltage microscope" and as a logarithmic voltmeter.*

Effect of the input network on the rejection factor

Where a potential difference between two points is to be measured, and a difference amplifier having a high rejection factor is used for this purpose because both points have a high voltage with respect to earth, careful attention should also be paid to the network by which the amplifier is coupled to the points in question. Any asymmetry in that network can ruin the results obtained with a good difference amplifier.

If the measurement is concerned solely with alternating voltages, the amplifier is usually coupled to the points by two capacitors, C and C' (*fig. 18*). Voltage division then occurs across these capacitors and across the input resistances R_i and R_i' of the amplifier. If the products R_iC and $R_i'C'$ are not equal, an in-phase component of E_i and E_i' gives rise to an anti-phase component in the voltage on the input terminals. This coupling network may then be said to have its own finite rejection factor. Provided the discrepancy is not too great, this factor is given by:

$$H = \frac{4\pi f R_i C}{\delta}, \quad \ldots\ldots \quad (17)$$

where f is the signal frequency and δ the relative difference between the products R_iC and $R_i'C'$. Using components for R_i, R_i', C and C' that may show a maximum deviation of 5% from the nominal value, the products R_iC and $R_i'C'$ may show a maximum discrepancy of 20% ($\delta_{max} = 0.2$). In this case the minimum value of the rejection factor is:

$$H_{min} = 20\pi f R_i C. \quad \ldots\ldots \quad (18)$$

Given the requirement $H_{min} = 50\,000$ at $f = 50$ c/s, for example, then the product R_iC must be at least equal to 16 seconds. If R_i and R_i' are rated at 1 MΩ, the capacitors used for C and C' must therefore have a rating of at least 16 μF.

This is a much higher value than would be needed for simply keeping the voltage drop in such a network reasonably low. Simple calculation shows that, for the input signals of the amplifier to differ by no more than 1% from E_i and E_i', the capacitance of C and C' under the conditions mentioned need be only 0.022 μF.

Another important quantity to be considered when using a difference amplifier is the internal resistance of the voltage sources that supply E_i and E_i'. Here too even a slight difference may reduce the rejection factor considerably. In *fig. 19* the internal

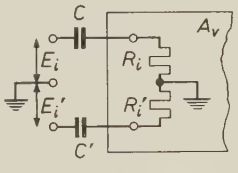

Fig. 18.

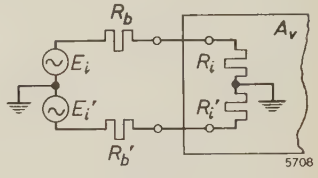

Fig. 19.

Fig. 18. Network for coupling a difference amplifier A_v to the points between which the potential difference is to be measured. Mutual disparities between C and C' and between R_i and R_i' can have a marked effect on the rejection factor.

Fig. 19. Connection of a difference amplifier A_v to two points regarded electrically as voltage sources having internal resistance R_b and R_b'. Any difference in these resistances may considerably reduce the rejection factor.

resistances of the signal sources are denoted by R_b and R_b'. The network sketched can again be said to have a rejection factor, which, if R_i and R_i' are identical and R_b and $R_b' \ll R_i$, is given by:

$$H = 2\frac{R_i}{\Delta R_b}. \quad \ldots\ldots \quad (19)$$

Here ΔR_b is the absolute value of the difference between R_b and R_b'. Where the amplifier is to be used for a variety of purposes, it must be taken into account that in some cases the internal resistance of one of the voltage sources, e.g. R_b', is zero. In that case ΔR_b is equal to the internal resistance of the other voltage source, and therefore:

$$H = \frac{2R_i}{R_b}. \quad \ldots\ldots \quad (20)$$

*) Research Laboratories, Eindhoven.
) Philips tech. Rev. **23, 142, 1961/62 (No. 5).

When R_b has a specified value, then in order to allow for this unfavourable situation the input resistances of the difference amplifier must be equal, according to (20), to at least:

$$R_i = \tfrac{1}{2} H R_b . \quad . \quad . \quad . \quad . \quad . \quad . \quad . \quad (21)$$

If R_b is 1 kΩ and the minimum acceptable rejection factor of the input circuit is 50 000, then according to (21) the input resistances R_i and R_i' must be at least 25 MΩ. A value of this order is nearly always to be found in DC amplifiers, where the grids of the first valves are directly coupled to the input terminals and where no grid leaks are necessary for these valves. In AC amplifiers, where capacitors are connected between the grids and the input terminals and therefore grid leaks must be used, special measures are sometimes needed in order to obtain the high input impedance required.

In practice, cases are frequently encountered where the rejection factor of the input network is governed both by coupling capacitors and by the internal resistance of the voltage sources. Here again, it is a fairly simple matter to calculate the values which the various resistances and capacitances must have in order to be able to guarantee a specific minimum rejection factor.

Multi-stage difference amplifiers

Hitherto we have been concerned solely with single-stage difference amplifiers. We shall now briefly consider various problems that arise in the design of multi-stage amplifiers. In a previous article [5]) it was shown that as a rule the rejection factor of a difference amplifier is primarily governed by that of the first stage. It should be noted that the rejection factor of a multi-stage amplifier can also be influenced by the coupling elements between the stages: asymmetry in these elements may reduce the rejection factor that can be guaranteed for a given circuit. The considerations applicable to the coupling elements between the stages are similar to those mentioned in regard to the circuit elements used for connecting the difference amplifier to the measuring points. Since lower demands are made on the part of the circuit following the first stage, however, the requirements are not so rigorous.

In AC amplifiers the stages are nearly always coupled in the conventional way by means of capacitors and resistors. In this case, then, the above remarks also apply to these circuit elements. In DC amplifiers, where coupling capacitors obviously cannot be used, the grids of the valves in the second stage can be directly connected to the anodes of the valves of the first stage (see *fig. 20*). In order for the second-stage valves to be biased to their normal operating point, their anodes and cathodes must have a higher potential than the corresponding electrodes in the previous stage. The higher supply voltages then needed may be felt as a drawback. To get around this difficulty, voltage dividers can be used for the coupling between the various stages (*fig. 21*), thereby lowering the "voltage level" of the second and successive stages. Of course, this has the effect of reducing the sensitivity of the amplifier. An even greater objection to the use of voltage dividers is that they increase the output resistances of the first stage and lower the input

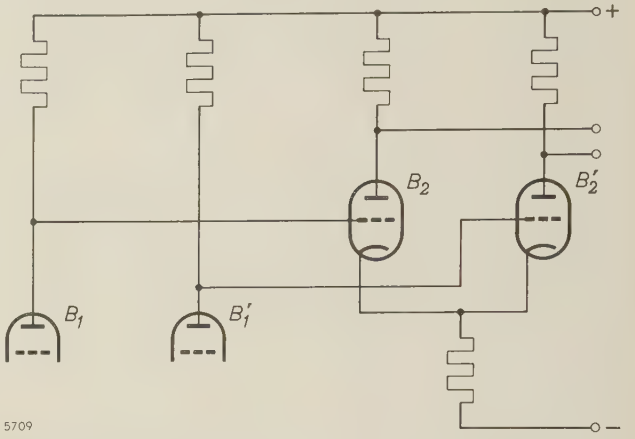

Fig. 20. Difference amplifier for DC voltages with direct interstage coupling.

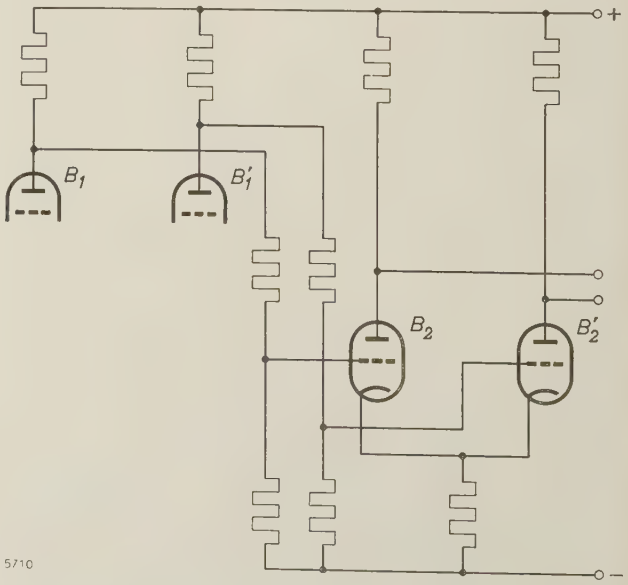

Fig. 21. Difference amplifier for DC voltages, with the two stages coupled via voltage dividers.

[5]) G. Klein and J. J. Zaalberg van Zelst, General considerations on difference amplifiers, Philips tech. Rev. **22**, 345-351, 1960/61 (No. 11).

resistances of the second stage; in connection with the mutual disparity between these resistances, the result is that the guaranteed rejection factor for the coupling network is lower (see eq. (20)). For this reason, in DC difference amplifiers where very high demands are made on H_{min} the grids of the valves in the second stage are frequently connected directly to the anodes of the valves in the first stage. In the further stages the coupling can be as shown in fig. 21 (see also fig. 26).

Reducing the DC voltage level without any appreciable loss in sensitivity can be achieved with a circuit using elements whose differential resistance is much higher than their DC resistance. A circuit of this type is shown in *fig. 22*. The elements having a very high differential resistance are formed

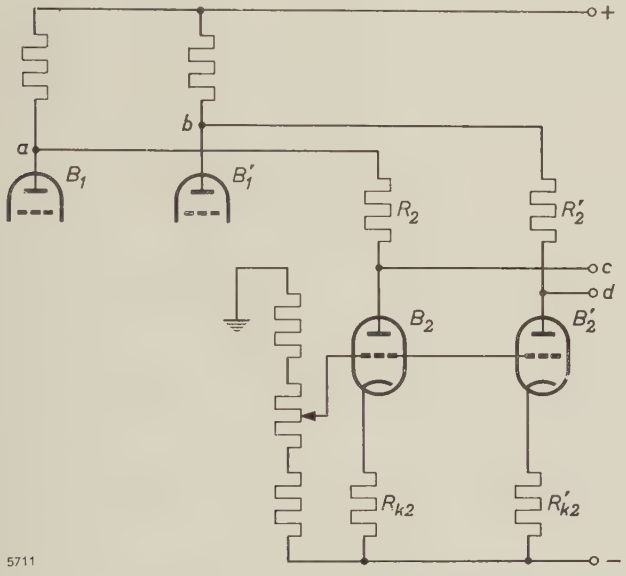

Fig. 22. Circuit in which the DC voltage level of points *c* and *d* is lower than that of points *a* and *b*, although there is scarcely any attenuation of the signal voltage.

by triodes B_2 and B_2' with resistances R_{k2} and R_{k2}' incorporated in the cathode leads. If the resistances R_2 and R_2' are small compared with these differential resistances, the voltage level of points *c* and *d* can be much lower than that of points *a* and *b*, although the signal voltages are passed with virtually no attenuation. An arrangement as sketched in fig. 22 can be used with particular advantage where the difference amplifier is required to deliver strong output signals, e.g. for deflecting the beam in a cathode ray tube. In this way it is possible to avoid the difficulties that may arise from the use of a voltage divider built up from normal resistors, owing to the fact that the last stage then has to supply a signal voltage several times higher than the voltage taken from the divider.

Gain control

When a difference amplifier is built up from several stages, gain control will generally be wanted. When choosing the appropriate circuit it should be borne in mind that the gain control too may reduce the rejection factor. For this reason it is usually inadvisable to apply the gain control to the first stage, the rejection factor of which has to meet the highest demands.

A widely used method of gain control — varying the transconductance of the valves by changing the negative grid bias — is not effective here in view of the high differential resistances in the cathode leads.

A severe drawback also attaches to the method represented in *fig. 23*. If it is used in a DC amplifier, its effect is also to alter the operating point of the valves in the next stage. Here too, the guaranteed rejection factor is lowered, owing to the mutual disparity in the voltage-division ratios of the potentiometers.

Fig. 24 indicates an arrangement with which the gain of the difference amplifier can be varied without altering the operating points of the valves. The gain for anti-phase signals is controlled by the variable resistance between the two anodes. This resistance does not, however, affect the gain for in-phase signals, and therefore the discrimination factor F varies in the stage whose gain is controlled. Consequently the rejection factor H of the next stage has to meet higher demands.

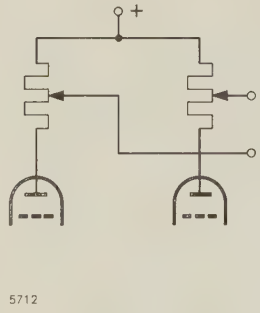

Fig. 23.

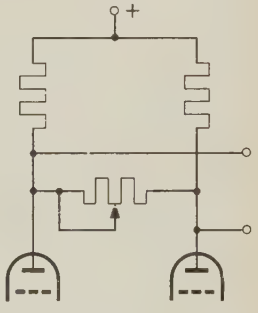

Fig. 24.

Fig. 23. Method of gain control. A discrepancy in the voltage-division ratios of the two potentiometers may result in a lower rejection factor. If this circuit is used in a DC amplifier, the setting of the gain control affects the operating point of the valves in the following stage.

Fig. 24. Method of gain control where the discrimination factor is dependent on the value of the variable resistance.

The same can be said of the circuit sketched in *fig. 25a*, where a variable resistance is inserted between the two cathodes. Here again, the magnitude of this resistance determines the gain for anti-phase signals, but has no influence on the gain for in-phase signals. Increasing the gain therefore again

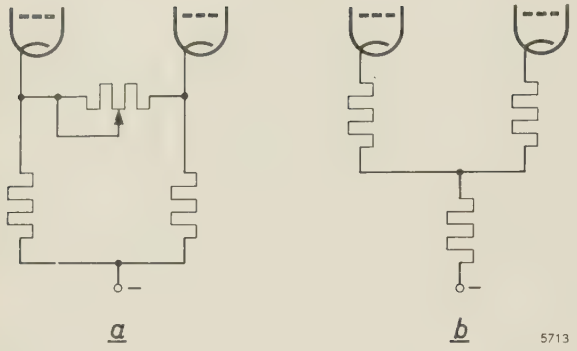

Fig. 25. *a*) Method of gain control, where both the discrimination factor and the rejection factor are dependent on the value of the variable resistance.
b) Equivalent circuit, with the delta resistance network replaced by a star network.

reduces the discrimination factor. Moreover, the variable resistance in this circuit can also influence the rejection factor. This can be seen most readily if we replace the delta network of resistances by an equivalent star network, as in fig. 25*b*. In this arrangement there is negative feedback as a result of the resistances in the cathode leads of the valves. These resistances are roughly equal to half the resistance between the cathodes in fig. 25*a*. The result of this negative feedback is to reduce the effective transconductance of the valves, which again reduces the guaranteed rejection factor. This network too should therefore preferably be applied to one of the last stages of a difference amplifier, where the rejection factor is not so critical.

As a further illustration of the methods of controlling the gain, *fig. 26* shows the circuit diagram of a 3-stage difference amplifier. The second stage contains a 3-step volume control as shown in fig. 24, and the gain of the third stage is controlled on the principle represented in fig. 25. Further particulars of this circuit will be found in the caption to the figure.

Influence of supply voltages; stability

In a sensitive, unbalanced amplifier designed for signals of very low frequency the constancy of the supply voltages, particularly for the first stage, is always an important consideration. A fluctuation in the anode supply voltage, for example, can produce a change in the output voltage from the valves in the first stage which is amplified by the following stages and thus occurs as an interference component in the amplified signal. It is important to note that, for a given sensitivity, the demands made on the constancy of the supply voltages for a difference amplifier need not be as high as in the case of a normal amplifier. This can be understood by considering a difference amplifier in its simplest form, with triodes whose control grids in the quiescent state are at earth potential (see fig. 1). A change in the positive and negative supply voltages by the same amount in the same direction, corresponds to an in-phase signal at the input terminals. This in-phase signal appears at the output terminals attenuated by the rejection factor with respect to the anti-phase signal to be amplified.

If only one of the two supply voltages changes, the effect on the output signal is not so simple to analyse. It can be shown that a change in the *positive* supply voltage of the first stage appears in the output signal as an anti-phase signal which is attenuated with respect to the input signal by a factor

$$\frac{2\mu^2}{\Delta\mu},$$

and that the corresponding factor for a change in the *negative* supply voltage is:

$$\frac{4SR_k}{\frac{\Delta S}{S}+\frac{\Delta R_a}{R_a}+\frac{1}{4}\frac{R_a}{R_k}\frac{\Delta\mu}{\mu^2}}.$$

From equation (5) we see that the sum of the reciprocals of these two factors is equal to $1/H$, which confirms the effect deduced above of a simultaneous change of both supply voltages in the same direction. Since the rejection factor is at least equal to H_{min}, both the above attenuation factors are always greater than the minimum value of the rejection factor.

More complicated circuits also involve auxiliary voltages, which are often derived for simplicity from the positive and negative supply voltages and are therefore affected by changes in the latter (see e.g. figs 10 and 11). It can be shown that the disturbances thus introduced are always a few orders of magnitude smaller than those occurring in an unbalanced amplifier.

As the thermionic emission of a valve depends on the *heater voltage*, and this dependency differs from one valve to another, changes in heater voltage will also appear at the output terminals as an anti-phase signal, obviously of very low frequency. The magnitude of this anti-phase signal depends on the construction of the valves, and its maximum value is therefore dependent on the type of valve used. Experiments with numerous valves have shown that in this respect the type E 80 CC triode gives the best results. It was found that in a difference amplifier fitted with this type of valve a change of

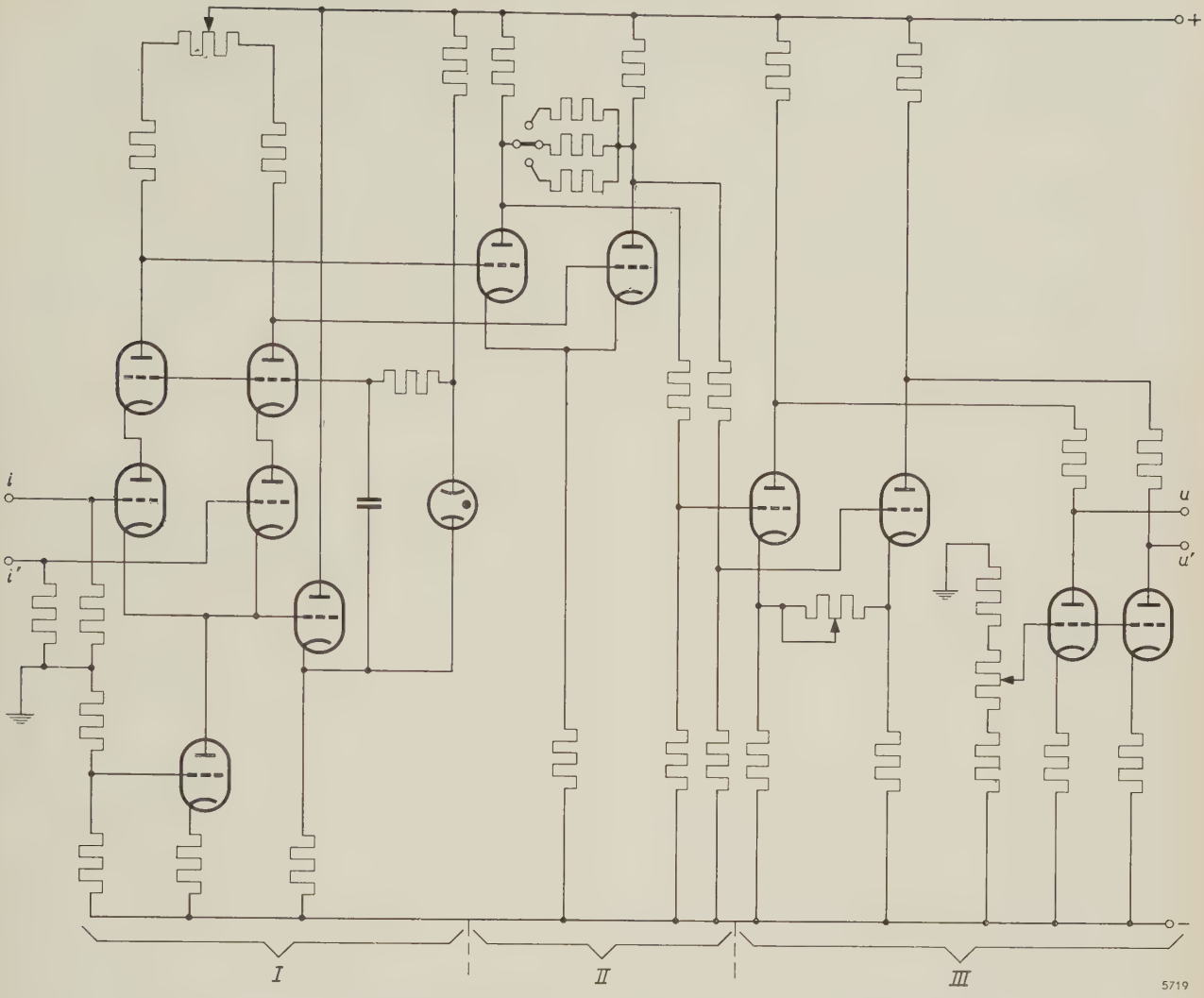

Fig. 26. Circuit diagram of a three-stage difference amplifier. The stages are denoted by *I*, *II* and *III*. Stage *I* is designed as in fig. 14; stages *II* and *III* are simple circuits, each with two amplifying triodes. Stages *I* and *II* are directly coupled (cf. fig. 20); stages *II* and *III* are coupled via voltage dividers to reduce the DC voltage level (fig. 21). Stage *II* uses three-step gain control as in fig. 24; the gain control in *III* is as in fig. 25. The output terminals are given earth potential in the quiescent state by the circuit shown in fig. 22. The different heights at which the valves are drawn correspond to the differences in their DC voltage levels.

10% in the heater voltage caused an interfering anti-phase signal the maximum value of which corresponded to an anti-phase signal of 10 mV at the input. Although this disturbance is small compared with the corresponding disturbance in an unbalanced amplifier (100 to 200 mV), it is still excessive in many cases. For difference amplifiers too, therefore, it may be necessary to ensure that the heater voltage remains reasonably constant, with variations considerably less than 10%.

Another complication frequently encountered with sensitive amplifiers is the occurrence of feedback via the supply circuit, which may even give rise to oscillation. In a *balanced amplifier* there is generally much less feedback of this kind than in an unbalanced amplifier, owing to the fact that the current variations in the output valves are in anti-phase and the supply circuit need therefore deliver hardly any current varying with the signals. A *difference amplifier* is even more favourable in this respect, because, as shown above, a signal voltage returned from the output via the supply circuit to one of the previous stages undergoes very little amplification.

To a considerable extent the advantages mentioned can often be obtained by designing only the *first stage* as a difference amplifier and the remainder as normal amplifying stages. The effect of supply-voltage fluctuations and any tendency to instability can frequently be substantially suppressed in this way. Usually, however, the full advantages of a difference amplifier are only obtained by designing the amplifier with *all* its stages as difference

amplifiers. Since the stages following the first stage can usually be fairly simple in circuitry, an entirely balanced amplifier may even in fact be simpler than an amplifier which is partly unbalanced.

The above-mentioned advantages of a difference amplifier enable such an amplifier to be used in cases where it is not a question of amplifying the voltage difference between two arbitrary points, but the potential of one point to earth. One of the two input terminals is then earthed (*fig. 27*) and the difference amplifier is used as a "normal" amplifier. The output voltage may be taken either in push-pull from the output terminals or between one of these terminals and earth, as desired.

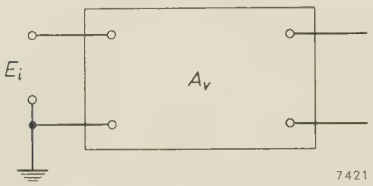

Fig. 27. Difference amplifier used as an unbalanced amplifier.

Negative feedback

It is easily seen that the discrimination factor of a difference amplifier is lowered if a simple form of negative feedback is introduced, the in-phase and anti-phase signals being returned in the same ratio from the output terminals to the input. Since the in-phase signals undergo much less amplification, the feedback also reduces the gain for these signals much less than for the anti-phase signals. In a difference-amplifier with negative feedback, then, the feedback ratio for in-phase signals should be much larger than for antiphase signals. Because of the interaction of in-phase and anti-phase signals, it is not so easy to see what effect the feedback has on the rejection factor. For this reason we shall not be concerned in this article with the problems arising from the use of feedback in a difference amplifier.

Quite another matter is the fact that a difference amplifier can be used as a means of producing highly effective negative feedback in an unbalanced amplifier. In this procedure a signal voltage derived from the output is returned in the usual way to the input stage of the amplifier, the aim being to amplify the difference between the input signal and the feedback signal. In a commonly used circuit the latter signal is applied to the cathode of the first valve, which then in fact functions as a difference amplifier. After what has been said it will be clear that the rejection factor of such a "difference amplifier" will as a rule be very small. Although the object of the feedback, i.e. to reduce distortion and minimize the extent to which the parameters of valves and other components influence the gain, may be satisfactorily achieved, better results are possible if a good difference amplifier is used as the first stage (see *fig. 28*). The feedback is then more effective, because the input signal and the feedback

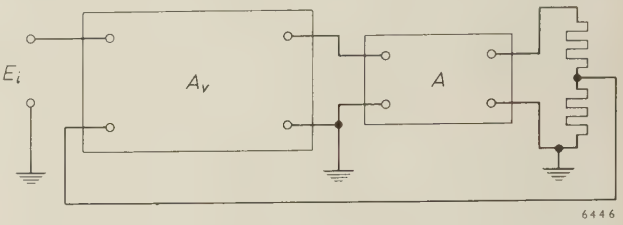

Fig. 28. Difference amplifier used as the first stage in a feedback amplifier.

signal contribute almost equally to the output signal. This also offers advantages in circuitry, since there is hardly any load on the feedback network and because the feedback signal can be applied to the first stage at earth potential.

The use of difference amplifiers with large anti-phase signals

Where high voltages are to be measured or otherwise investigated, the use of a high-gain amplifier is seldom considered. Nevertheless a sensitive difference amplifier offers advantages here that are not so easily obtained by other means. To make this clear, we should first of all point out that in the above theory on the operation of a difference amplifier we assumed that the anti-phase signal on the grids is small enough to allow a reasonable current to flow in both valves, this signal then being amplified as in a conventional balanced amplifier. There is no amplification, however, if the anti-phase signal exceeds the above-mentioned limit, for in that case the anode current in one of the valves is cut off, with the result that the other valve functions as an unbalanced amplifier with a very high cathode impedance. The gain of this valve is then extremely low. It may further be said that a difference amplifier gives amplification only when the difference in potential between the two input terminals does not exceed a specific value. As soon as this potential difference exceeds that value the difference amplifier is "overdriven". This does not mean, however, that the valves are overloaded. If the input signal of a multi-stage amplifier is progressively increased, it will generally be the valves in the last stage that are "overdriven" first, since it is here that the signals are strongest. If the gain for anti-phase signals is high, only a small potential difference between the input terminals is sufficient to overdrive the last stage. The amplifier may be so designed, for exam-

ple, that amplification occurs only if the potential difference between the input terminals amounts to no more than a few millivolts, and if necessary even less.

This property of a difference amplifier can occasionally be turned to good use, particularly for the purpose of very accurately comparing two differently time-dependent signals at the moments when they are almost identical. Suppose, for example, that the one input voltage, E_i, is a DC signal and the other, E_i', a large AC signal (see *fig. 29*),

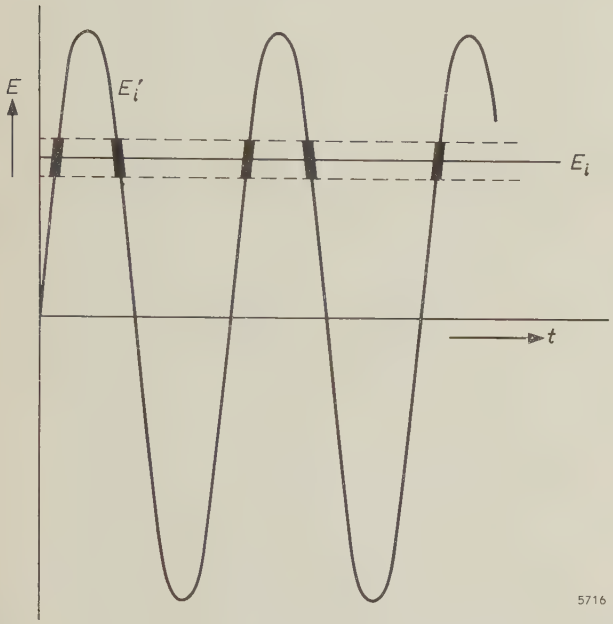

Fig. 29. Amplitude-versus-time plot of the voltages E_i and E_i' on the input terminals of a difference amplifier when the latter is used in combination with an oscilloscope as an "electronic voltage microscope". Only the thickly outlined portions of E_i' are displayed on the oscilloscope.

then the latter signal will only be amplified at the moments at which its instantaneous value differs only very slightly from the magnitude of the DC signal. By connecting the output of the difference amplifier to an oscilloscope, very small portions of the waveform of the alternating voltage can then be displayed distinct from the remainder of the wave form. The portions concerned are drawn thick in fig. 29. The combination of a difference amplifier and oscilloscope in this way may be described as an "electronic voltage microscope". Using a high-gain difference amplifier, it is thus possible to display a detail of a few millivolts of a waveform whose amplitude is ten or more volts. If E_i is made roughly equal to the peak value of E_i', the "voltage microscope" displays only the peaks of the AC signal (*fig. 30*). This constitutes a highly accurate method of checking the constancy of the signal amplitude. *Fig. 31* shows an example of such an

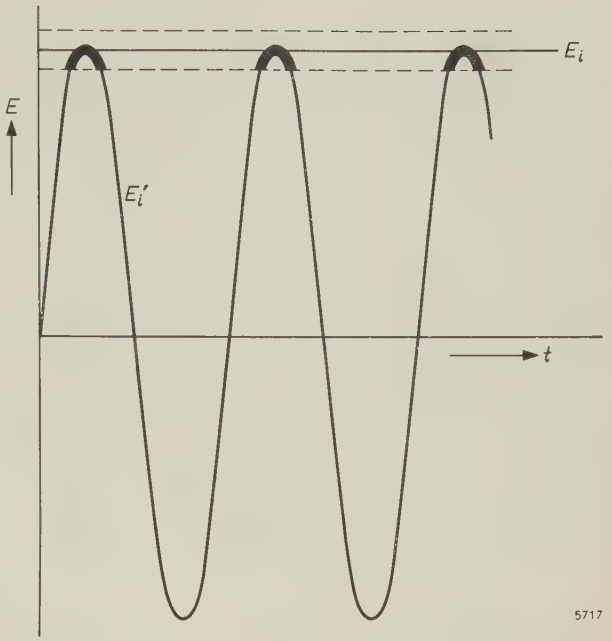

Fig. 30. When the DC voltage E_i is made roughly equal to the amplitude of E_i', only the peaks of E_i' appear on the oscilloscope.

oscillogram, obtained by applying to one input terminal of the difference amplifier an alternating voltage of 10 V amplitude and 80 c/s frequency, and to the other a DC voltage of 10 V. The height of a square in the figure corresponds to 2 mV. It can be seen that amplitude variations of roughly 4 mV occur, i.e. 0.04%. *Fig. 32* shows the top portion of a 10 V square-wave voltage. We see here that the tops are not perfectly flat but show variations in amplitude of about 2 mV, i.e. 0.02%.

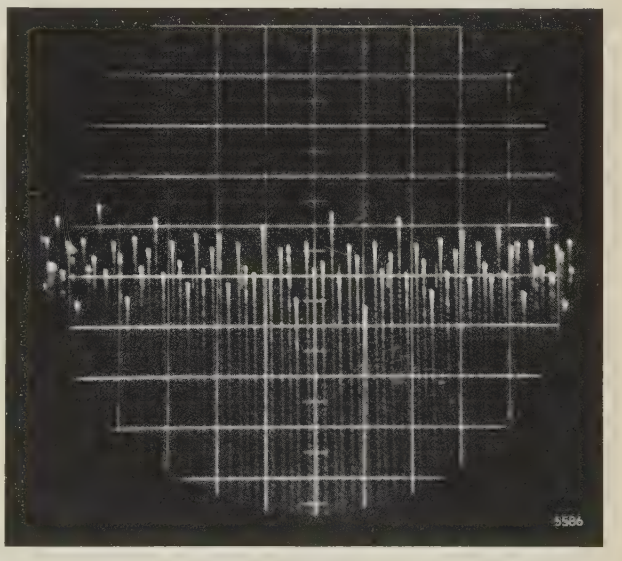

Fig. 31. Oscillogram obtained with a "voltage microscope" used to investigate an AC signal of amplitude 10 V. Only the peaks are displayed. The height of each square on the screen corresponds to 2 mV, so that in order to display the whole waveform the paper would have to be 35 m in height! Very small variations in amplitude can be demonstrated in this manner.

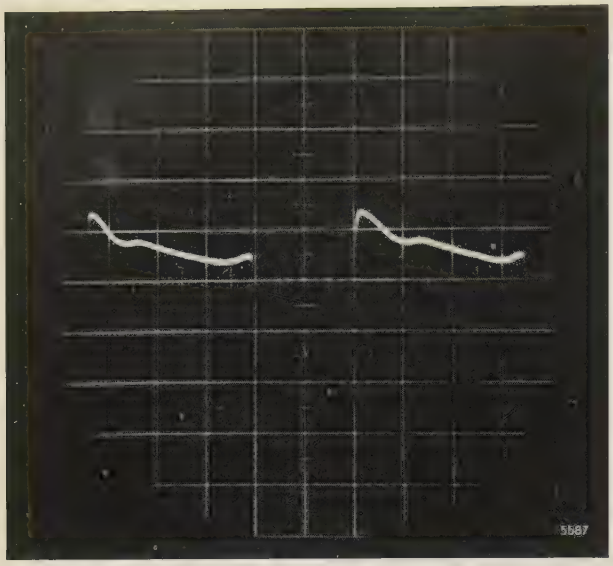

Fig. 32. Top of a 10-V square-wave voltage. One square corresponds in height to 2 mV. The tops are not flat but show variations in amplitude of roughly 2 mV.

Since a DC voltage can as a rule be measured directly with greater precision than an AC voltage (e.g. using a compensator), a difference amplifier also makes it possible to determine the amplitude of an AC signal in a very accurate but simple manner. The procedure is simply to make E_i equal to the amplitude of the AC signal to be measured, E_i', as illustrated in figs 30 and 31, and to measure E_i.

To conclude, we shall describe another application of a difference amplifier where a high DC voltage E_i is applied to one input terminal and a periodically varying voltage E_i' is applied to the other. In fig. 29 the waveform of E_i' is sinusoidal, but we shall now assume that E_i' is a different periodic function of time. As an example, it is assumed in *fig. 33* that E_i' decays exponentially in each cycle:

$$E_i' = E_{i0}' \, e^{-\frac{t}{T_0}}, \quad \ldots\ldots \quad (22)$$

where T_0 is a constant.

Anode current now flows in both valves of the last stage only as long as the signal voltage on the grid of the relevant valve is greater than that on the grid of the other valve. During these times the anode currents are practically constant; the output signal E_o of the difference amplifier thus has a square-wave form, as shown in fig. 33 below. A simple calculation shows that the mean value E_{om} of E_o is a logarithmic function of E_i:

$$E_{om} = \frac{E_1}{T}(2T_0 \ln E_{i0}' - 2T_0 \ln E_i - T) \quad \ldots \quad (23)$$

(E_1 and T are explained in fig. 33). The value E_{om}, measured with an integrating circuit, is a measure of E_i on a logarithmic scale, and the whole arrangement thus constitutes a *logarithmic voltmeter.*

If E_i' is a periodic exponentional function of time, we thus obtain an output signal whose mean value is the *inverse* (logarithmic) function of E_i. It is not difficult to see that, even if E_i' is some other periodic function of time, this method still produces an output signal which is the inverse function of E_i. This can be turned to use in various ways [6]).

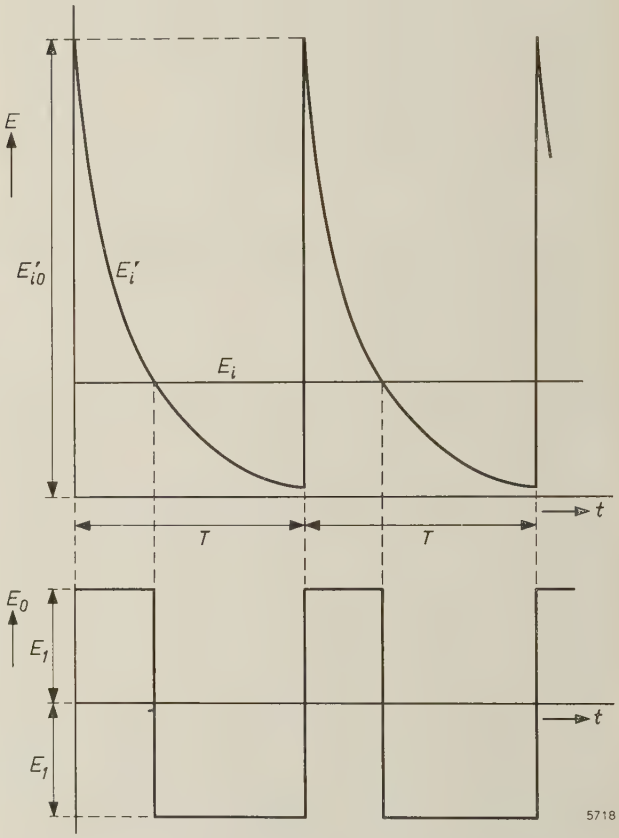

Fig. 33. Use of a difference amplifier as a logarithmic voltmeter. *Above:* The two input signals, E_i and E_i', as functions of time. *Below:* Output signal as a function of time.

Without going deeper into these and other possible applications of difference amplifiers, it is hoped that the above examples have shown that there are many more uses for these amplifiers than simply the amplification of small potential differences.

[6]) See G. Klein and J. M. den Hertog, A sine-wave generator with periods of hours, Electronic Engng. **31**, 320-325, 1959.

Summary. The minimum value of the rejection factor of a difference amplifier is affected by the elements coupling the amplifier to the points between which the potential is to be measured. In a multi-stage amplifier, the coupling elements between the stages also have an important influence. An incidental advantage of a difference amplifier compared with normal types is that less rigorous demands are made on the constancy of the supply voltage; a difference amplifier also shows much less tendency to oscillate. Further applications for difference amplifiers are discussed, in particular as a means of introducing highly effective feedback in an unbalanced amplifier, as an "electronic voltage microscope" and as a logarithmic voltmeter.

INSPECTION OF NEGATIVES FOR PRINTED CIRCUITS

Photo Maurice Broomfield

Inspection of a master negative used in the manufacture of printed circuits by the photographic etched-foil process. Prints of this negative are made on a copper-plated panel of laminated board coated with photographic emulsion. The unexposed parts of the copper foil are removed by etching. This method lends itself particularly well to the reproduction of fine detail. Since the slightest fault is reproduced in the finished product, the negatives are subjected to careful scrutiny all the time they are in use.

RADIATION FURNACES OF PAST CENTURIES

662.997:621.472

The carbon-arc image furnace, whose use as a laboratory instrument is described in this issue (page 161), has had numerous predecessors. The use of lenses or concave mirrors to focus the sun's rays for lighting kitchen fires or altar flames was known to antiquity [1]). In the 16th and 17th centuries radiation furnaces had found a place in the equipment of metallurgists and alchemists. In 1540 Biringuccio [2]) mentioned a mirror roughly a foot in diameter with which a gold ducat could be melted. Glauber [3]) in c. 1650 indicated the size of mirror required for specific purposes: 1 span (= 9 inches) for igniting wood, 2 spans for melting tin, lead and bismuth, 4 or 5 spans for melting gold and silver and also for forging iron. Robert Hooke even planned to base a kind of temperature scale on this scheme.

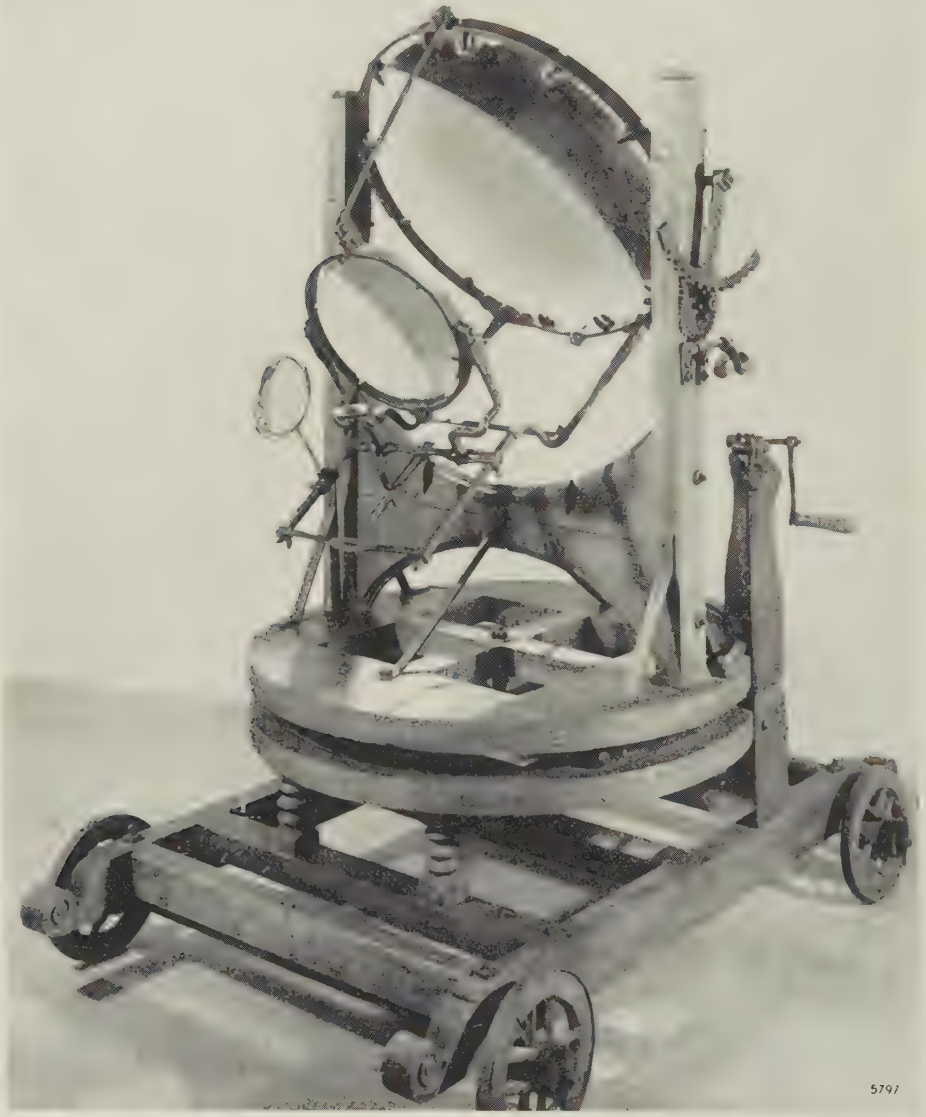

Fig. 1. Burning-glass instrument built by E. W. von Tschirnhaus towards the end of the 17th century. (Reproduced by courtesy of the Deutsches Museum, Munich.)

[1]) Various sources are mentioned by R. J. Forbes, Studies in ancient technology, VI, Brill, Leyden 1958.
For some of the particulars mentioned here we are indebted to Professor Forbes personally.

[2]) V. Biringuccio, De la Pirotechnia libri X, Roffinello, Venice 1540.

[3]) J. R. Glauber, Opera mineralis, Amsterdam 1651.

At the end of the 17th century, the century in which the first lens systems for telescopes had been built and considerable progress made in the grinding of lenses, mirrors were for a time outstripped by lenses. This was largely due to the work of the German mathematician and physicist E. W. von Tschirnhaus (1651-1708) [4]). He had occupied himself with the improvement of "burning mirrors" since 1679, and in 1687 he is reported to have made a gigantic mirror 130 cm in diameter, beaten from sheet copper. He then apparently realized that he could do better with lenses than with the imperfectly focussing mirrors (the art of grinding parabolic mirrors had not yet been perfected), which were moreover difficult to handle. He set up a glass works, where larger pieces of glass were cast than any one had managed to do before, he developed special grinding methods, and he hit on the idea of combining a large lens with a smaller one (the "collective"), which improved focussing. In February 1694 he stated in a letter to Leibniz that he had succeeded in melting with his lenses several substances which were previously considered to be unmeltable. Among these substances was clay; this discovery enabled him to make porcelain, which had been imported from China for centuries but which no one in Europe had previously known how to imitate [5]).

Tschirnhaus' great lens systems were greeted with much enthusiasm, and were sold to physical societies in various European countries, where they were used for scientific or pseudo-scientific ends. One went to Holland, apparently (Leibniz wrote about it to Huygens in 1694); Tschirnhaus sent two to Paris — one of them with an enormous lens 94 cm in diameter and weighing 74 kg; other lenses went to London, St. Petersburg etc. Several of these lens systems are preserved. The Lomonosov Museum in Leningrad still houses the lens of the equipment Tschirnhaus had sent there, with a diameter of 57.5 cm and still in its original wooden housing. The Mathematisch-Physikalische Salon in Dresden also has several pieces of Tschirnhaus equipment [6]). But particularly well preserved is the complete Tschirnhaus "burning glass" in the Deutsches Museum, Munich, which is shown in *fig. 1*. This has an objective lens 75 cm in diameter.

A somewhat smaller instrument (objective lens about 37 cm diameter) is to be found in the Museo di Storia della Scienza in Florence [7]). Benedetto

[4]) For the details given below see especially: J. S. T. Gehler, Physikalisches Wörterbuch, Leipzig 1787, and the more recent publication: R. Wunderlich, Brenngläser als Hilfsmittel chemischen Forschens, Chymia **2**, 37-43, 1949.

[5]) E. W. von Tschirnhaus, De magnis lentibus seu vitris causticis eorumque usu et effectu, Acta eruditorum (Leipzig) 1697, pp. 414 et seq.

[6]) For details see: E. W. von Tschirnhaus und die Frühaufklärung in Mittel- und Osteuropa, Ed. E. Winter, Akademieverlag Berlin 1960, especially the articles by O. Volk (pp. 247-265) and V. L. Cenakal (pp. 285-307).

[7]) Maria L. Bonelli, The burning glass of Benedetto Bregans of Dresden, "Florence" **11**, No. 2, p. 22, 1960.

Fig. 2. Mezzotint engraving by John Chapman after a painting by Richard Corbould from 1805, symbolizing the Science of Chemistry at the crossroads. The chemist in the background is demonstrating the preparation of oxygen by decomposition of an oxide in a solar furnace. (Reproduced by courtesy of Prof. John Read, University of St. Andrews, Scotland. See: J. Read, The alchemist in life, literature and art, Nelson, London 1947.)

Bregans brought this from Dresden in 1690; it thus probably came from Tschirnhaus' workshop, too. In 1710 Bregans presented his burning glass as a gift to Grand Duke Cosimo III of Tuscany. It is interesting to note that the Florence instrument was put to use a century later for a scientific investigation undertaken by Humphrey Davy and his assistant at that time, Michael Faraday. Davy and Faraday visited Florence in 1814, and Davy profited from the opportunity to use the burning glass for studying the the experiment in his diary. His report begins: "Today we made the grand experiment of burning the diamond, and certainly the 'phenomena presented were extremely beautiful and interesting". The diamond in the experiment was placed in a perforated platinum crucible in the middle of a glass sphere filled with pure oxygen (volume 22 cubic inches). Under the heat of the solar image produced by the "Duke's burning glass" for three quarters of an hour — with interruptions to cool the glass

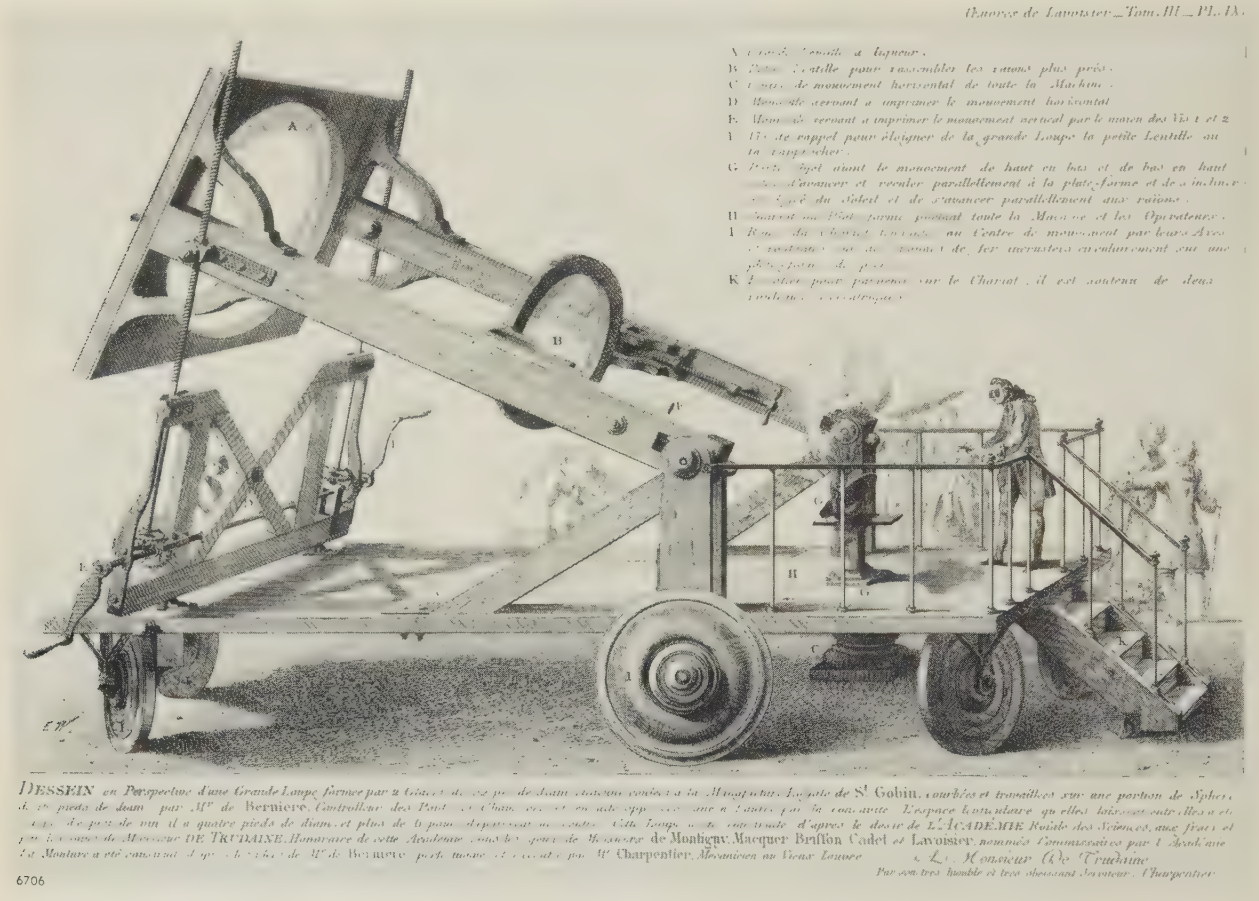

Photo Deutsches Museum, Munich

Fig. 3. Etching by Charpentier from 1775, showing the burning device with a great liquid lens built in 1774 to order of the Académie Royale des Sciences, Paris, for the investigations of Lavoisier *et al.* The lens consisted of two spherically curved cast-glass plates which fitted closely together, the space between them (4 feet in diameter, more than 6 inches thick in the middle) being filled with alcohol, and later with turpentine. (From: Oeuvres de Lavoisier, Vol. III, Paris 1865.)

combustion of diamond — a subject which had already occupied Cosimo III, and which Lavoisier *et al.* had thoroughly investigated starting in 1772, partly with the aid of the Tschirnhaus burning glass in Paris [8]). Faraday gave a detailed description of sphere — the diamond seemed gradually to shrink and become opaque, and finally caught fire, whereupon it burnt away in a few minutes without further heating.

The etching reproduced in *fig. 2*, after a painting by Corbould from 1805, gives a nice idea of what the experiment described may have looked like. At that time the science of chemistry was on the threshold of a new era, the phlogiston theory of combustion

[8]) See Abbé Rozier, Observations sur la Physique, sur l'Histoire Naturelle et sur les Arts, Vol. 2 (1772), pp. 108-111 ("Résultat de quelques expériences faites sur le diamant par MM. Macquer Cadet et Lavoisier de l'Académie Royale des Sciences").

having just been discredited. The picture shows Chemistry, allegorically represented as a beautiful maiden wearing a coronet, hesitating between the old and the new, symbolized as age and youth. The young chemist is demonstrating the preparation of oxygen in a solar furnace using a lens system. This experiment was done in a very similar way by Priestley [9]) — himself still an obstinate supporter of the phlogiston theory — in 1775.

The burning glass had beaten the concave mirrors for a while, because the mirrors were even more difficult to make, and more difficult to handle: it was found to be virtually impossible to keep the mirrors continually focussed on the object to be heated in long experiments. It was however realized that the performance of the burning glasses was limited by their chromatic and other aberrations and by the optical flaws in the great masses of glass. In order to eliminate these flaws in the glass, the Académie Royale des Sciences commissioned a big *liquid lens* (*fig. 3*) for Lavoisier *et al.* as late as 1774. But by that time the technique of grinding *parabolic* mirrors was beginning to be mastered (J. Short 1710-1768, W. F. Herschel 1738-1822 [10])), and although, as we have seen above, use was still made of the existing solar furnaces using burning glasses for a long time, the days of the picturesque big lens systems were drawing to a close.

S. GRADSTEIN *).

[9]) J. Priestley, Philosophical Transactions Vol. **65**, 1775, letters of 15th March, 1st April and 29th May. The burning glass used by Priestley is still preserved at Dickinson College, Carlisle, Pa. (U.S.A.).

[10]) An interesting alternative was developed by Buffon, who showed in 1747 that a large number of suitably arranged *flat* mirrors could be used instead of a concave mirror (Kircher had put this idea forward in 1646), and that the same experiments could be done with these as with the great burning glasses. He managed to melt a silver object at 20 feet with an arrangement of 117 mirrors. An arrangement of this type used by Buffon is preserved in the Conservatoire des Arts et Métiers, Paris. This method is again being used today, notably for a gigantic Russian installation for making use of solar energy.

*) Research Laboratories, Eindhoven.

ABSTRACTS OF RECENT SCIENTIFIC PUBLICATIONS BY THE STAFF OF N.V. PHILIPS' GLOEILAMPENFABRIEKEN

Reprints of those papers not marked with an asterisk * can be obtained free of charge upon application to Philips' Electrical Ltd., Century House, Shaftesbury Avenue, London W.C. 2, where a limited number of reprints are available for distribution.

2870: K. Reinsma: The inherent filtration of X-ray tubes (Radiology **74**, 971-972, 1960, No. 6).

If the inherent filtration of an X-ray tube is known, it is possible to determine the extra filtration required to reach the prescribed total. For a given voltage the radiation quality of an X-ray beam, expressed in mm Al half-value layer, depends markedly on the waveform of the voltage (constant potential or full-wave rectified). Further, there is a marked difference in the equivalent inherent filtration, depending on whether it is determined from dose measurements or from the radiation quality. For the latter case, a set of curves is given showing radiation quality as a function of equivalent inherent filtration (mm Al) for various voltages from 50 to 150 kV constant potential, and 50-100 kV full-wave rectified.

2871: H. F. L. Schöler, E. H. Reerink and P. Westerhof: The progestational effect of a new series of steroids (Acta physiol. pharmacol. neerl. **9**, 134-136, 1960, No. 1).

In order to study the influence of stereochemical changes upon the pharmacological properties of steroids, a number of steroid hormone analogues have been prepared which have the same configuration of the C-9 hydrogen atom and the C-10 methyl group as present in lumisterol$_2$ (see No. **2856**). The activities of the compounds administered subcutaneously and orally at three dosage levels were compared with that of progesterone administered subcutaneously, also at three dosage levels. Photographs taken of the uterine sections were ranked according to the degree of change in the shape of the mucous-membrane epithelium.

2872: F. C. de Ronde, H. J. G. Meyer and O. W. Memelink: The *P-I-N* modulator, an electrically controlled attenuator for mm and sub-mm waves (IRE Trans. on microwave theory and techniques **MTT-8**, 325-327, 1960, No. 3).

The construction and performance of a millimetre-wave modulator are described. The main part of the

modulator consists of a *P-I-N* germanium structure inserted into a rectangular waveguide. A modulation depth of 11 dB could be obtained at frequencies up to 5 kc/s, this modulation being caused for the greatest part by attenuation.

2873: H. C. Hamaker: Attribute sampling in operation (Bull. Inst. Int. Statistique **37**, 265-281, 1960, No. 2).

The features of practical interest in attribute sampling procedures are discussed and on the basis of the arguments brought forward some modifications in existing sampling tables are proposed which, it is believed, would render these tables of still greater practical value. Some of the topics considered are sample size efficiency, the AQL (acceptable quality level) concept, the relation between lot size and sample size, advantages of a constant sample size, and tightened and reduced inspection. At the end the main conclusions are summarized and a modified sampling standard is proposed as a basis for discussion.

2874: B. Okkerse: De bereiding van dislocatievrije germaniumkristallen (Ingenieur **72**, O 21 - O 26, 1960, No. 29). (The preparation of dislocation-free germanium crystals; in Dutch.)

The paper gives a method for the preparation of dislocation-free germanium crystals. Dislocations in germanium crystals are generated by sources which are activated by the thermal stresses during the growth of the crystal. By decreasing the diameter of the seed crystal to about 1 mm these stresses can be reduced. Consequently the seed crystal can be made dislocation-free, and then a dislocation-free crystal may grow on this seed crystal. The relevant properties of dislocations and various techniques for detecting dislocations are reviewed. Some properties of dislocation-free germanium crystals are discussed. See also Philips tech. Rev. **21**, 340-345, 1959/60.

R 411: J. H. N. van Vucht: Ternary system Th-Ce-Al (Philips Res. Repts **16**, 1-40, 1961, No. 1).

A report of an investigation of the ternary system Th-Ce-Al, including a review of data on the binary systems Th-Al, Ce-Al and Th-Ce and on the element cerium. No ternary compounds were found in the system Th-Ce-Al. This investigation was primarily undertaken to determine the structure of "Ceto", a non-evaporating getter; this structure is described.

R 412: P. C. Newman, J. C. Brice and H. C. Wright: The phase diagram of the gallium-tellurium system (Philips Res. Repts **16**, 41-50, 1961, No. 1).

The phase diagram of the gallium-tellurium system has been investigated by differential thermal analysis and direct observation of melting points under controlled tellurium pressures. The results of these investigations, which are confirmed by X-ray analysis, show that besides the two compounds already known (GaTe and Ga_2Te_3), there exist two other compounds Ga_3Te_2 and $GaTe_3$. These two compounds, however, are not stable at room temperature. A hexagonal unit cell for $GaTe_3$ with $a = 6.43$ Å and $c = 14.20$ Å is reported. The melting points of GaTe and Ga_2Te_3 are 835 ± 2 °C at 6×10^{-2} torr Te-pressure and 792 ± 2 °C at 2 torr, respectively. Upper decomposition limits for Ga_3Te_2 and $GaTe_3$ are 753 ± 2 °C and 429 ± 2 °C.

R 413: J. D. Fast and M. B. Verrijp: Internal friction in lightly deformed pure iron wires (Philips Res. Repts **16**, 51-65, 1961, No. 1).

The internal friction (damping of free torsional vibrations) of pure (99.99%) iron wires is measured before and after they have been subjected to a very small plastic deformation. The damping after deformation is found to be strongly dependent on the amplitude of the deformation, the temperature at which it was carried out, and the temperature of measurement. Wires which are deformed at temperatures below —30 °C show a spontaneous increase of damping with time, while those deformed at higher temperatures show a spontaneous decrease. In the latter case the logarithm of the damping is found to be a linear function of t^p, where t is the time and p a constant between 0.2 and 1.0 which varies from experiment to experiment. Further experiments carried out with increased concentrations of vacancies and carbon atoms have shown that the spontaneous decrease of the damping is due to the diffusion of point defects towards dislocations, and the anchoring of the latter by the former. The spontaneous increase of the damping is probably due to the dispersion of local concentrations of dislocations.

R 414: L. Schmieder: The behaviour of the mercury high-pressure arc under mechanical vibrations (Philips Res. Repts **16**, 66-84, 1961, No. 1).

If a high-pressure mercury-vapour lamp is allowed to vibrate sinusoidally in a direction perpendicular to the axis of the discharge, the arc voltage rises. If both the frequency and the velocity amplitude of the vibration exceed certain values, the arc will be quenched. This can be explained by assuming that the mechanical vibration gives rise to forced

gas flow, which results in a certain loss of energy from the arc by convection. If the lamp is suddenly given a (constant) acceleration, it takes some time before the resulting Poiseuille flow pattern becomes constant. This transient time explains the existence of a critical frequency for the quenching of the discharge. Above this frequency, the gas behaves like a frictionless fluid because of its inertia. The convection losses are then proportional to the velocity amplitude of the mechanical vibration. The "mechanical stability" of the arc is defined as the velocity amplitude needed to quench the arc at frequencies above the critical frequency. Calculations show that this quantity is proportional to the diameter of the tube and inversely proportional to the mass of gas per unit length of tube. The experimental results agree quite well with these calculations.

R 415: J. A. W. van der Does de Bye: Signal-to-noise ratio of a *p-n*-junction radiation counter (Philips Res. Repts **16**, 85-95, 1961, No. 1).

X-ray quanta can be counted with the aid of a *P-N* diode of low capacitance, biased in the reverse direction. The quanta give rise to pairs of holes and electrons in the space-charge layer between the *P* and *N* regions. The charges on these particles can be completely collected and measured, thus making X-ray spectroscopy possible. This paper deals chiefly with the influence of the noise on the detection of the signal produced with the aid of a thermionic amplifier with *RC* pulse shaping. For a given choice of the circuit involved, the noise is mainly determined by the diode current I_g and the shot noise of the first amplifier tube. The quantity $C^2R_{eq}I_g$, where C is the total input capacitance and R_{eq} the equivalent noise resistance of the first amplifier tube, may be used as a quality factor for the *P-N* counter. This quality factor can be used to calculate the minimum quantum energy at which detection of X-rays is possible (6 keV) and the width of the spectral lines (3 keV), i.e. the minimum energy difference between two quanta which can still be distinguished. The experimentally determined values were 9 and $4\frac{1}{2}$ keV respectively.

R 416: M. Koedam: Cathode sputtering by rare-gas ions of low energy (Philips Res. Repts **16**, 101-144, 1961, No. 2).

It is well known that a metal emits atoms when it is bombarded with gas ions; this phenomenon is known as cathode sputtering. It was first observed, more than a hundred years ago, in a gas discharge between two (cold) electrodes. This thesis (Utrecht, March 1961) describes measurements carried out with mono-energetic gas ions striking the metal surface at right angles. The energy of the ions varied between 40 and 1500 eV. Chapter I contains a summary of the most important literature. Chapter II describes the apparatus, and some measurements carried out to determine the energy distribution of the gas ions. Chapter III is devoted to the determination of the number of atoms released by the cathode sputtering. After a summary of previous methods follows a detailed description of the method used in the present investigation: the sputtered metal is collected on a glass plate, and the amount determined from the optical transmission of glass plates plus metal layer. This chapter also contains a comparison of the structure of layers of silver (and copper) formed by sputtering and by evaporation. The experimental results are given in chapter IV. The sputtering yield (atoms/ion) was determined as a function of the energy of the gas ions (which varied between 40 and 250 eV) for polycrystalline silver. The angular distribution of the sputtered atoms was determined for monocrystalline copper bombarded with gas ions of energies up to 1500 eV. It was found that the ⟨110⟩ and ⟨100⟩ directions are preferred directions, while the angular distribution also depends on the nature and energy of the bombarding ions. The experimental results are discussed and compared with those of other authors in chapter V. The existence of preferential directions for the sputtering and the variation of the angular distribution with the ion energy are explained.

R 417: A. J. W. Duijvestijn and A. J. Dekkers: Chebyshev approximations of some transcendental functions for use in digital computing (Philips Res. Repts **16**, 145-174, 1961, No. 2).

Description of iterative methods for finding the best approximation to continuous functions in a given interval by means of a truncated polynomial or a truncated continued fraction. The article also describes direct methods for obtaining approximations to such best approximations.

R 418: B. H. Schultz: On the study of volume recombination of excess charge carriers in semiconductors with the aid of photoconductance (Philips Res. Repts **16**, 175-181, 1961, No. 2).

A method is described for the elimination of surface effects in determinations of the recombination time of holes and electrons in semiconductors by means of photoconductance measurements. More-

over, the measurements indicate directly whether the value found for the recombination time is reliable or not.

R 419: B. H. Schultz: Recombination at copper and at nickel centres in *p*-type germanium (Philips Res. Repts **16**, 182-186, 1961, No. 2).

The rate of recombination of excess holes and electrons at copper centres in germanium depends on the temperature. If the germanium also contains some antimony, which partially compensates the acceptor action of the copper, a different dependence on the temperature is found. All the experimental results can be explained by assuming that recombination occurs not only at copper ions, but also at neutral copper atoms. The contradiction between the results obtained by previous workers is hereby resolved. A similar contradiction which is also found with nickel could not be resolved. The data obtained in the present investigation agree with those of Wertheim, but not with those of Kalashnikov and Tissen.

R 420: L. J. van der Pauw: Determination of resistivity tensor and Hall tensor of anisotropic conductors (Philips Res. Repts **16**, 187-195, 1961, No. 2).

The resistivity tensor of an anisotropic conductor with respect to an arbitrarily chosen rectangular coordinate system can be described by six constants. It is shown that these six constants are related to the "sheet resistivities" of six plane-parallel samples by six linear equations. The plane-parallel samples may be of arbitrary shape and cut in arbitrary but known directions. The Hall effect can most generally be described by nine constants. For the determination of these nine constants only three such samples are required, combined however with three different orientations of the magnetic induction.

H 9: K. Böke: Kapazitätsmessungen an der Grenzfläche Silicium-Elektrolyt (Z. Naturf. **15a**, 550-551, 1960, No. 5/6). (Capacitance measurements on silicon-electrolyte interfaces; in German.)

A short report of capacitance measurements on the interface between silicon and an electrolyte. These experiments form part of a fundamental investigation of the phenomena occurring at the surface of semiconductors. See also **H 10**.

H 10: H. U. Harten: The surface recombination on silicon contacting an electrolyte (Phys. Chem. Solids **14**, 220-225, 1960).

A silicon disc of thickness equal to the recombination length for diffusion is immersed in an electrolyte. A voltage applied between the electrolyte and the sample is used to vary the charge density on the surface of the silicon. The rate of surface recombination and the surface photoelectric effect are measured as functions of the applied voltage. The results are in qualitative agreement with the theory, and are dependent on the oxidation state of the silicon.

H 11: G. Schulten and H. Severin: Dämpfungsarme Leitungen für Millimeterwellen (Nachr. techn. Fachber. **23**, 20-23, 1961). (Low-damping transmission lines for millimetre waves; in German.)

A brief survey of surface-wave transmission lines, which can have considerably lower attenuation for millimetre waves than the more common type of waveguide in which the wave is propagated in the interior of a hollow conductor.

H 12: H. Severin: Neuere Mikrowellenferrite und ihre Anwendungen (Nachr.techn. Fachber. **23**, 24-27, 1961). (New microwave ferrites and their uses; in German.)

A brief survey of ferrites which can be used at higher and lower frequencies in the microwave region than has been hitherto possible. A number of factors determining the upper and lower frequency limits for such applications are discussed.